Algorithms for Adolescent Idiopathic Scoliosis Classification Based on Surface Topography Analysis

by

Maliheh Ghaneei

A thesis submitted in partial fulfillment of the requirements for the degree of

Master of Science
in
Structural Engineering

Department of Civil and Environmental Engineering
University of Alberta

Abstract

While the common method for diagnosing and monitoring adolescents with idiopathic scoliosis (AIS) is X-ray radiographs from which a Cobb angle is measured, studies have shown that high radiation exposure is linked to high risk of cancer, particularly, for children and women. This thesis describes an algorithm for AIS classification based on surface topography analysis which is a radiation-free method.

We present an approach which improves the user-independence level of the previously developed 3D markerless asymmetry analysis using a new asymmetry threshold without compromising its accuracy in identifying the progressive scoliosis curves. Thresholds, which have been used for separating the deformed area, were changed to automatically isolate the deformed area paired with Cobb angles. New classification trees were developed to use asymmetry parameters for classifying curve severity and progression status. In monitoring of scoliosis curves progression over a period of 12±3 months, the sensitivity of curve progression was increased from 68% to 75%, while the specificity was decreased from 74% to 59%, compared with the original method. Results demonstrate that smaller number of radiographs would be saved, however the risk of missing a curve with progression would be decreased, i.e. the proposed approach is more conservative in monitoring of scoliosis curves in clinical applications.

Although using the classification tree method led to promising results, it was highly sensitive to threshold values selected in the decision trees. We demonstrate another classification algorithm, custom Neighbourhood Classifier, by which the accuracy of the curve severity and progression were increased by 17% and 58%, respectively. The new algorithm is based on the idea that curves with close asymmetry parameters are likely to belong to the same class. Regarding the contribution of each asymmetry parameters, in general, they do not play the same role in decision making, thus modification was performed to use such parameters properly.

Preface

Some of the research conducted for this thesis forms part of a research collaboration led by Dr. Samer Adeeb at the University of Alberta.

The setup of technical apparatus and surface topography data acquisition was completed by Dr. Eric Parent research group.

Chapter 2 of this thesis has been submitted to the Journal of Medical & Biological Engineering & Computing as M. Ghaneei, A. Komeili, Y. Li, E. Parent, S. Adeeb, “3D Markerless Asymmetry Analysis in the Management of Adolescent Idiopathic Scoliosis”. I was responsible for the analysis as well as the manuscript composition. Dr. A. Komeili, Dr. Y. Li, Dr. E. Parent, and Dr. S. Adeeb were involved with concept formation.

Chapter 3 of this thesis has been submitted to Journal of Computer Methods in Biomechanics and Biomedical Engineering as M. Ghaneei, R. Ekyalimpa, L. Westover, E. Parent, S. Adeeb, “Customized k-Nearest Neighbourhood Analysis in the Management of Adolescent Idiopathic Scoliosis Using 3D Markerless Asymmetry Analysis”. I was responsible for the analysis as well as the manuscript composition. Dr. R. Ekyalimpa, L. Westover, Dr. E. Parent, and Dr. S. Adeeb contributed in concept formation.

This thesis is an original work by Maliheh Ghaneei. The research project, of which this thesis is a part, received research ethics approval from the University of Alberta Research Ethics Board, Project Name “Full Torso Asymmetry Analysis for Scoliosis”, Pro00040500, 2016.

During the last two years, the following conference papers were published:

1- Eric C. Parent, Maliheh Ghaneei, Samer Adeeb, Sanja Schreiber, Marc Moreau, Douglas Hedden, Douglas Hill, Sarah Southon (2016). Effects of Schroth Exercises

Added to Standard Care in Adolescents with Idiopathic Scoliosis (AIS) on Marker-less Surface Topography Asymmetry Measurements – A Randomized Controlled Trial (RCT). 1ST Joint SOSORT-IRSSD Education and Scientific Meeting, Banff Canada, (Podium-Presented)

2- Maliheh Ghaneei, Eric C. Parent, Samer Adeeb (2016). Improving Marker-less Surface Topography Asymmetry Measurements for Adolescents with Idiopathic Scoliosis (AIS). 2nd Annual Structures Graduate Students Conference, Edmonton Canada, (Podium-Presented)

3- Maliheh Ghaneei, Eric C. Parent, Samer Adeeb (2016). Improving Marker-less Surface Topography Asymmetry Measurements for Adolescents with Idiopathic Scoliosis (AIS). Glenrose Rehabilitation Hospital Spotlight on Research Breakfast Poster Symposium, Edmonton Canada, (Podium-Presented).

4- Maliheh Ghaneei, Eric C. Parent, Samer Adeeb, Sanja Schreiber, Marc Moreau, Douglas Hedden, Douglas Hill, Sarah Southon (2016). Effects of Schroth Exercises Added to Standard Care in Adolescents with Idiopathic Scoliosis (AIS) on Marker-less Surface Topography Asymmetry Measurements. 10th Annual WCHRI Research Day, Edmonton Canada, (Poster)

5- Maliheh Ghaneei, Eric C. Parent, Samer Adeeb (2017). Automatic Patch Isolation in The Asymmetry analysis of Surface Topography for Adolescents Idiopathic Scoliosis. The 23rd Congress of the European Society of Biomechanics, Seville Italy, (Podium-Presented)

To my husband, Mahdi,
who is always a constant source of support
and to my parents and my sisters for their unconditional love.

Acknowledgements

I would like to gratefully express my appreciation towards my supervisor Dr. Samer Adeeb who kindly gave me the opportunity to investigate my research interest and guided me patiently to the destination through his invaluable supports and assistance in the friendly and peaceful environment. I am heartily thankful to him, whose encouragement, fast response and being always available, no matter it is weekend or late at night, were significant inspiration in my academic journey.

I am also grateful to have Dr. Eric Parent as a clinical scientist. He always willingly shares his expertise with me when I need it the most. His editorial assistance in writing the manuscripts made the outcome of my research more practical in the clinic.

I would like to thank Dr. Yong Li, Dr. Amin Komeili and Dr. Ronald Ekyalimpa for their collaboration, careful reading and minute criticism of my thesis.

I proudly acknowledge the financial support I have received from my supervisor, Scoliosis Research Society (SRS), the Faculty of Graduate Studies and Research (FGSR), the Graduate Students Association (GSA) at the University of Alberta and Women and Children's Health Research Institute (WCHRI).

I would like to thank all my friends and colleagues with whom I have spent a wonderful time while studying towards my M.Sc. program.

My deepest thanks and appreciation go to my parents, Maryam and Hossein, who have always encouraged me to follow my dreams. They never stopped caring and motivating me with my goals from so far away. My warmest gratitude goes to my lovely sisters, Mahboube and Zakiye, and my brother-in-law, Farshid, who kindly support me throughout my life and studies.

Last but not least, it is my pleasure to gratefully thank my best friend and husband, Mahdi, for his invaluable understanding, endless support and pure love.

Table of Contents

List of Tables

List of Figures

List of Acronyms

ΔCA	Change of Cobb angle
ΔMaxDev	Change in maximum deviation of the colour patch
ΔRMS	Change in root mean square of the colour patch deviation
2D	Two Dimension
3D	Three Dimension
AIS	Adolescent Idiopathic Scoliosis
L	Lumbar
MaxDev	Maximum deviation of the colour patch
PA	Posterior Anterior
RMS	Root Mean Square of distances between matched points
ST	Surface Topography
T	Thoracic
TL	Thoracolumbar
k-NN	k Nearest Neighbourhood

1

Introduction

1.1 Motivation

Adolescent Idiopathic Scoliosis (AIS) is the most common form of scoliosis affecting children and predominately girls. Studies have shown that high radiation exposure is linked to high risk of cancer [1]. Furthermore, such risk is higher for those exposed as children or women. Given that the common way to assess the severity of the scoliosis or its changes over the time is using radiographs, a practical method was required to reduce the exposure to X-ray radiations. Thus, Surface topography (ST) has been introduced, a method in which only harmless visible light is used to replace radiographs. The ST method has evolved through the contribution of various studies resulting in remarkable improvements, however still some limitations exist [2] Recent ST analysis is based on the asymmetry of the torso and represents decision trees to classify the severity of the curvature and its progression [3]. Due to the limitations of the previous studies which caused inaccurate results in evaluating torso asymmetry in some cases, to the best of our knowledge, there still exists a considerable need to improve the method. The desired method should be fully automated to make the whole process repeatable, fast, and easy enabling its full clinical implementation. Once implemented, the proposed method would prevent adolescents with a mild AIS status or no progression in their spinal curve from being exposed to unnecessarily radiation.

1.2 Literature Review

1.2.1 Scoliosis

Scoliosis is a 3D deformity of the spine caused by lateral deviation greater than 10 degrees as measured using the Cobb angle method obtained from radiograph scans in the standing position. This deformity is usually combined with axial rotation of the vertebrae [4]

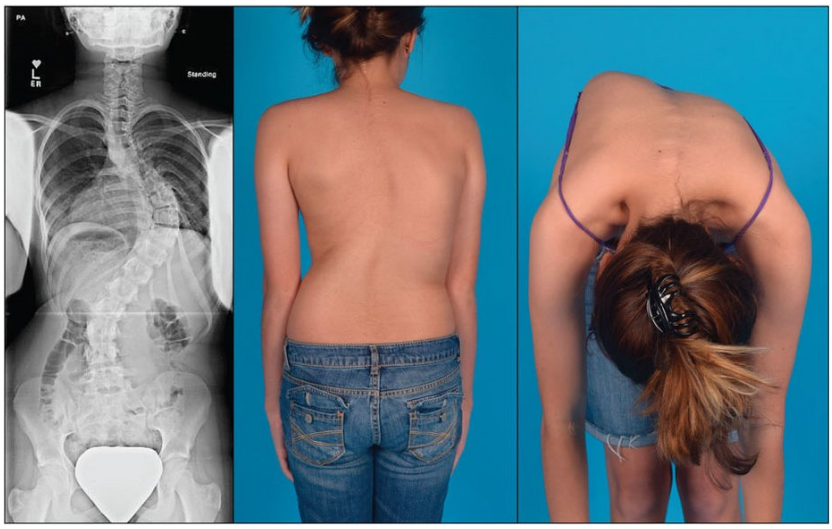

Figure 1-1- Idiopathic Scoliosis in an adolescent female [5] (Figure is licensed under CC by 4.0)

Scoliosis is classified in different groups based on the age of the patients at the time of diagnosing. Infantile, juvenile, and adolescent are detected before 3 years old, 3 to 10, and 10 years old to skeleton maturity, respectively [6]. The term “Idiopathic” means the specific cause of this phenomenon is still unknown, although according to some studies, it could be a genetic disorder [6, 7]. 80% of patients with scoliosis are diagnosed with adolescent idiopathic scoliosis and most of them are female [9]. For instance, for curvatures greater than 30 degrees, girls are affected 10 times more than boys. Furthermore, scoliosis curve progression in girls is faster requiring them to receive more treatment [6].

1.2.2 Radiographs

As mentioned before, Cobb angle is the most widely used method in scoliosis clinics to assess the severity and progression of AIS based on X-ray radiographs [10]. Cobb angle is a “Gold standard” that represents the angle between the most tilted vertebras above and below the scoliosis curve [11] (Figure 1-2). Following such definition, scoliosis is categorized into three levels: Mild (10°≤ Cobb angle ≤25°), Moderate (25°< Cobb angle ≤40°), severe (40°< Cobb angle). Additionally, progression is defined when there is over 5° increase in Cobb angle from baseline to follow-up [12].

Patients receive treatments based on the severity condition and progression status [13], i.e. mild patients may need check-ups every 3 to 9 months to see if they have any changes in their spine curvature. Additional treatments such as bracing are recommended for moderate curves to prevent further progression. In the worst case scenario, i.e. severe condition, orthopaedic surgery is the last resort for correction and stabilization of the spine [13, 14].

The main limitation of Cobb angle method is that the measurement is based on the posterior-anterior (PA) radiographs in which only the lateral deformation is visible. However, some patients may have axial rotation in their spine, so the 3D characteristics of the curves is not captured in this two-dimensional method. Another major drawback of using X-ray is the increase in the risk of cancer, which is intensified by the frequent X-ray monitoring and then young age of patients. Moreover, according to Hoffman *et al.* [1], the risk of breast cancer for women who were exposed to the X-rays because of scoliosis monitoring is doubled.

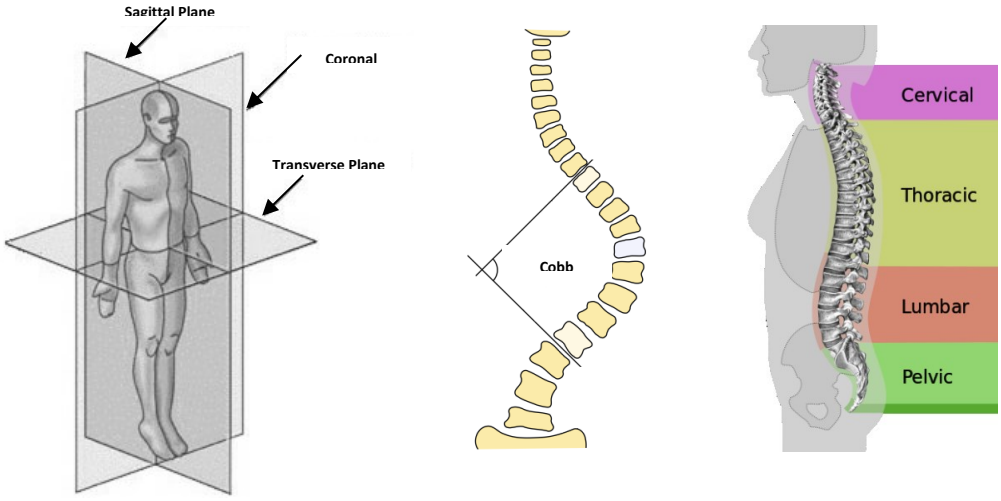

Figure 1-2- Measuring the Cobb angle [16,17, 18]

1.2.3 Surface Topography

Cosmetic deformity and its impacts on the quality of life are the preeminent reasons for patients with scoliosis to visit clinicians and seek improvement. The asymmetry associated with scoliosis is more annoying for them than having curved spine[15, 16]. Hence, these considerations highlighted the importance of assessing the appearance of the torso. Furthermore, the limitations of the Cobb angle method, as described before, motivated researchers to develop a method in which no X-ray is used and the 3D shape of the torso surface is investigated [21]. To that end, Surface topography (ST) was introduced as a non-invasive method which uses harmless visible light to capture the 3D scans of the torso. Several types of ST have been developed and in most of them there is a need to place landmarks in multiple anatomic locations to obtain the parameters involved in the analysis. These parameters are based on the coordinates of the landmarks with respect to each other and the geometric properties of the transvers cross section of the torso [18, 19]. These parameters are then used to calculate measures such as cosmetic score [24] and Quantec spinal angle [25] which can be used to assess the deformation or progression. ST studies have shown promising results in investigating torso deformity, however relying on trained operator which results in introduction of human errors in marker placement, is always a

controversial issue. Moreover, the limited number of anatomical points to place markers as well as lack of agreements on defining the aforementioned indices does not allow for studying the entire torso deformity [4]. These shortfalls prevent utilization of ST as a common method for diagnosing and monitoring scoliosis in clinics around the world.

More recently, Komeili *et al.* [26] introduced a markerless ST analysis method based on the asymmetry of the torso along the sagittal plane rather than landmarks, overcoming the limitations of marker placements [26]. In this technique, they defined a sagittal best plane of symmetry to create a deviation contour map which perfectly depicts the asymmetry areas, termed contour patches, affected by scoliosis (Figure 1-3). Best plane of symmetry is the plane that minimizes the distances between the actual points on the torso and its reflection. Maximum standard deviation (*MaxDev*) and root mean square of deviation (*RMS*) for each patch were two asymmetry parameters that were used to obtain clinical relation between the aforementioned parameters and the Cobb angle. Komeili *et al.* [3] suggested decision trees for diagnosing AIS and assessing curve progression based on the *MaxDev*, *RMS* and curve type. Hong *et al.* [27] independently validated the diagnostic accuracy of these trees for classifying mild curves and non-progression cases using a new set of AIS patients [28]. The results imply that patients with mild curves or those whose curves do not progress can be spared from being exposed to X-rays. Hong *at al.* [27] also modified the original decision trees to obtain more conservative results. While their classification tree has a good accuracy in detecting moderate/severe cases from mild patients (SE=73%), the percentage of mild patients who were eliminated from having unnecessarily X-rays was still low (SP=44%). In addition, all markerless ST analysis processes were automated to eliminate any human errors during the analysis except for the patch isolation step which was done manually in all the previous studies. Patch isolation was recognized as a complex process since previous attempts to automate this process resulted in merging between patches leading to inaccurate asymmetry results. However, manual isolation also resulted in varying *RMS* estimates. Moreover, in some patients, patches were extended all around the torso and it was hard to distinguish where the exact curvature of the spine is. Therefore, there is a need to

modify the process and properly define the patches so that they can be automatically isolated.

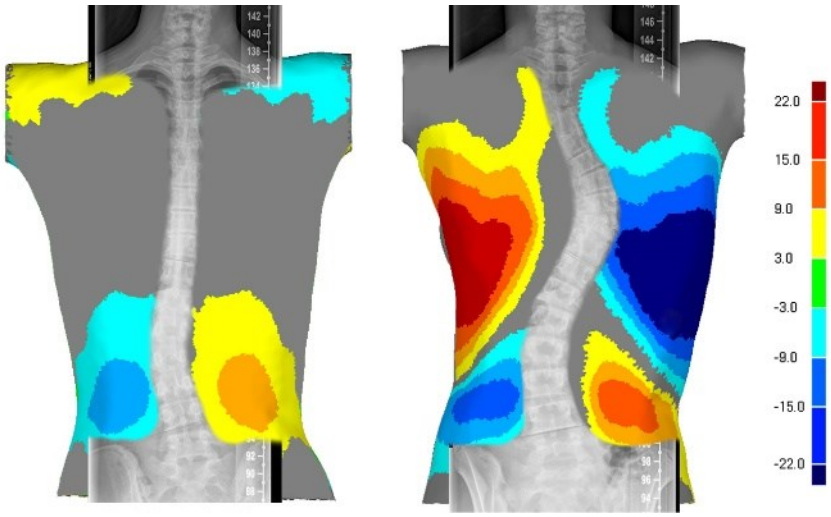

Figure 1-3- Isolated colour patch of two torsos with the corresponding radiograph [29]

1.2.4 Classification

The clinical relevance of radiograph measurements in evaluation of patients with AIS, in addition to the misperception in defining the degree of the scoliosis curve, underlines the necessity for the development of a classification system. Categorizing scoliosis patients to different groups helps clinicians better communicate and guides them in scoliosis management. Two main factors need to be considered to achieve promising classification, the first factor is determination of the most informative variables and the second one is the classifier technique itself.

According to Roudys, the first classification rule was proposed by Fisher in 1936 in statistical classification literature, after which other classification models were proposed and applied [30]. Classification is an example of a machine learning algorithm which uses experience to solve a given problem. Classification is defined as the process of identifying the group or category to which a new observation belongs, based on its qualities or characteristics. There are several classification algorithms, common examples include:

- Linear classifiers e.g. Logistic regression: A discrete or dichotomous (mild or moderate/severe) outcome can be predicated using such method where the variables could be continuous, discrete and dichotomous. The main idea of the method is that it defines the relationship between dependent variables and the dichotomous outcome [30, 31, 32, 33].
- Random forests (RF): The random forest as one can expect from the name is based on multiple decision trees rather than one tree, in which the training dataset is selected randomly, and each tree would work on some subsets of such data. The computation feasibility and accuracy of such method for various data domains are the significant features of the method [35].
- Learning vector quantization (LVQ): The underlying principle of learning vector quantization is to classify test data based on a set of pre-trained vectors. Similar to other machine learning algorithms first a random set of vectors is picked up and then is exposed to training samples. Next the vectors are trained based on the level of their similarities to a given pattern and can be further adjusted to acquire the desired result. Once the prototype vectors are fully trained they form the distribution in input space which can be used to classify samples from dataset [36].
- k-nearest neighbour (k-NN): One of the simplest and most common rule is Nearest Neighbourhood (NN). The main idea of NN is intuitive, which specifies that points with close parameters are likely to have same class, i.e. to classify a new query point, the class of nearest stored data points should be chosen. Although it is a simple algorithm, it has many advantages compared to the other methods such as decision trees and neural nets. For instance, stored data points can be gradually increased by adding more data points in the future. However, the main limitations of the NN are the dependence on the distance metric for classifying the new point and using all the stored data points for the analysis which is time consuming especially in a large database. Various approaches have been proposed to solve these issues. For example, the k-nearest neighbour (*k-NN*) algorithm is one of the common and simple extensions where input parameters are used to determine the k closest stored data points and then map them to an output through a systematic classification or a regression process, i.e. instead of analysing all the training instances, the k nearest neighbours are used. In this method, the value of k is

determined by minimizing the overall probability of error and all the independent parameters have equal contributions in the decision-making process [37]. k-NN algorithm was purposed more than 50 years ago but it got more popular in recent years due to the development of computers which can provide large memory for computations at a cheaper price [38]. Due to its simplicity, the k-NN is one of the most widely used algorithms [39]. Dasarathy is one of the textbook on nonparametric estimation and contains many papers using k-NN [40].

However, in medical diagnosis similar to many other applications the overall error probability is not the only or most important target and the key objective is increasing the confidence in the classification. Furthermore, for some particular classes of interest even higher confidence might be required compared to the rest of the classes. For instance, in AIS diagnosis, detecting a moderate/severe case is of crucial importance. Regarding the contribution of each independent variable, in general they do not play the same role in decision making, thus modification is required to utilize such parameters properly. Hence, in this study, the *k-NN* was modified to meet the requirements of the diagnosing and monitoring of AIS patients.

1.3 Thesis Objectives

The main objective of the present thesis is to address following problems in detail:

1- To modify the patch isolation method to automate the process of the markerless ST analysis
2- To validate the method using new set of data
3- To apply k-Nearest Neighbourhood classifier analysis to use markerless ST analysis for diagnosing and monitoring AIS

1.4 Thesis Outline

This thesis presents algorithms for AIS classification based on ST analysis and is organized as follows.

The modified 3D markerless asymmetry technique is described in Chapter 2. The selection criteria of the examined subjects, the description of our acquisition system and the asymmetry analysis technique are described in Section 2.3. The results of the asymmetry analysis for the torso of patients with AIS and comparison of the results with the original work are given in Section 2.4.

The Customized k-NN algorithm is given in Chapter 3. Section 3.3.2 presents the theoretical framework of the new classification approach. Section 3.4 presents the results of the conducted method and the comparison with the results of chapter 2.

Finally, Chapter 4 reviews the achievements of this study and presents the conclusion. This chapter also discusses the future work arising from this study.

2

3D Markerless Asymmetry Analysis in the Management of Adolescent Idiopathic Scoliosis[1]

2.1 Abstract

In an earlier study, a 3D markerless asymmetry analysis was developed to assess and monitor the scoliosis curve. While the developed surface topography (ST) indices demonstrated a strong correlation with the Cobb angle and its change over time, it was reported that the method requires user input for some patients. Therefore, this study aimed at improving the user-independence level of the previously developed 3D markerless asymmetry analysis using a new asymmetry threshold without compromising its accuracy in identifying the progressive scoliosis curves. A retrospective study was conducted on 128 patients with scoliosis with baseline and follow-up radiograph and ST assessments. The suggested cut point, that separated the deformed surfaces of the torso from the undeformed regions, automatically generated deviation patches corresponding to scoliosis curves for all analyzed ST

[1] This chapter has been submitted to Medical and Biological Engineering and Computing Journal, Maliheh Ghaneei, Amin Komeili, Yong Li, Eric Parent, Samer Adeeb.

scans. In monitoring of scoliosis curves progression, the sensitivity to curve progression was increased from 68% to 75%, while the specificity was decreased from 74% to 59%, compared with the original method. These results lead to a more conservative approach in monitoring of scoliosis curves in clinical applications; smaller number of radiographs would be saved, however the risk of missing a curve with progression would be decreased.

Keywords: Scoliosis, surface topography, 3D markerless asymmetry analysis, monitoring, curve progression

2.2 Introduction

Adolescent idiopathic scoliosis (AIS) is the most common form of three-dimensional (3D) spinal deformity. It affects 2–4% of the population, predominantly females [41]. The AIS spine deformity progresses rapidly during the adolescent growth period, resulting in a need for frequent follow-ups [42]. The gold standard for assessing the spine curve is measuring the Cobb angle on the full torso radiograph, with the Cobb angle defined as the angle between the two most tilted vertebrae in each curve [11].

The conventional scoliosis monitoring using the Cobb Angle has critical limitations recognized in the literature. Firstly, the measurement is limited to 2D posterior-anterior radiographs, and thus the method fails to address the 3D characteristics of AIS [43]. In addition, the use of radiographs in scoliosis clinics has several pitfalls of growing concern, such as excessive X-ray radiation exposure, with their associated risk of developing cancers [1, 30-33], and the contra-indication of radiograph acquisitions for pregnant women.

Surface topography (ST) was introduced to develop a new approach or enhance the existing scoliosis monitoring approach [30, 34, 35, 36]. ST is a method for which non-invasive visible light is used for scanning the torso surface in order to assess cosmetic deformities often based on some landmarks placed on the patient's torso by

trained clinicians and using related indices [3, 16, 18, 37, 38]. Measurements based on ST could possibly be used effectively in combination with the radiographs to decrease the radiation dose and risk of cancer resulting from the multiple X-ray acquisitions. At this point, the ST approach is by no means designed to fully replace the gold-standard radiograph measurements, because it is subject to validation with the radiograph measurements. Nevertheless, the development of accurate ST methods has significantly contributed to the management of scoliosis [3].

On the other hand, marker placements can be associated with human errors in collecting the raw data [4] and such methods fail to take into account the whole torso geometry in the analysis. In contrast, our team has developed a novel markerless ST asymmetry analysis approach, which is independent of human interactions, and considers the full 3D torso surface for the analysis [53] This technique provides a deviation contour map that visualizes the areas affected by AIS corresponding to the location of each curve, called deviation patch [3] These patches are isolated to calculate ST parameters for such deviations. The method demonstrated the potential for reducing 43% of radiograph exposure in the monitoring of scoliosis [29].

In the study presented by Komeili et al. [3], areas with deviation less than 3 mm were considered normal and areas with greater deviations were considered scoliosis deformation and separated as deviation patches for further analysis. Further application of this proposed ST asymmetry analysis in over 250 AIS patients illustrated that in 30 cases the method failed to either locate the curve properly or to correlate to the corresponding scoliosis curve, and led to misclassification of the AIS severity or progression. For example, in the ST analysis of some patients with a double scoliosis curve, a single isolated deviation patch encompassed the entire back torso (see Figure 2-2), and therefore did not reflect the double scoliosis curve in the corresponding radiograph. In some other cases, the deviation patch extended to the anterior part of the torso due to the asymmetry introduced by the breasts or axial rotation of the torso. Folded skin near the armpits and waist also introduced artifact in the ST analysis. The reasons for such lack of correspondence between the surface and the radiographic results were traced to the patch isolating stage. So far, these cases have been manually handled case by case by a scoliosis professional, which can introduce human

errors in the measurements and decrease the correlation between the ST parameters and radiograph measurements.

This study aimed to eliminate patch overlaps by enhancing the patch isolation procedure, and to increase the accuracy of the analysis in identifying patients where we could prevent unnecessary X-ray exposure (mild patients and those who did not experience any progression from the last visit). Our hypothesis is that the modifications suggested in this study would eliminate the manual step of isolating the deviation patches without compromising the accuracy of the method in monitoring the scoliosis curve severity or progression.

2.3 Materials and Methods

2.3.1 Data Collection

Full-torso ST scans of 128 AIS patients were collected from the Edmonton Scoliosis Clinic database between October 2009 and 2012. In the cohort, 95 patients (76 females, 19 males) had both baseline and follow-up ST and radiograph scans obtained with an interval of 12±3 months. The inclusion criteria used were patients aged 10 to 18 years old (14.4±1.8 years), with Cobb angle greater than 10° (26.5°±11.4°) at baseline, with no spine operation.

To develop a classification tree in order to identify the curve severity, 128 baseline radiograph and ST scans were used. In this sample, 99 thoracic-thoracolumbar (T-TL) curves and 98 lumbar (L) curves were measured, with double curves accounting for the larger curve count than the number of patients.

To classify the progression of the scoliosis curve, a sample of 95 ST and radiograph scans with corresponding follow-up scans were used, in which the progression of 137 curves in total were analyzed. The data sets were randomly divided into two groups (i.e., the Training group and the Validation group) as illustrated in

Figure 2-1. The training group included 80% of curves and was used in the derivation of the classification tree, whereas the validation group included the other 20% of curves and was used to examine the validity of the obtained classification tree.

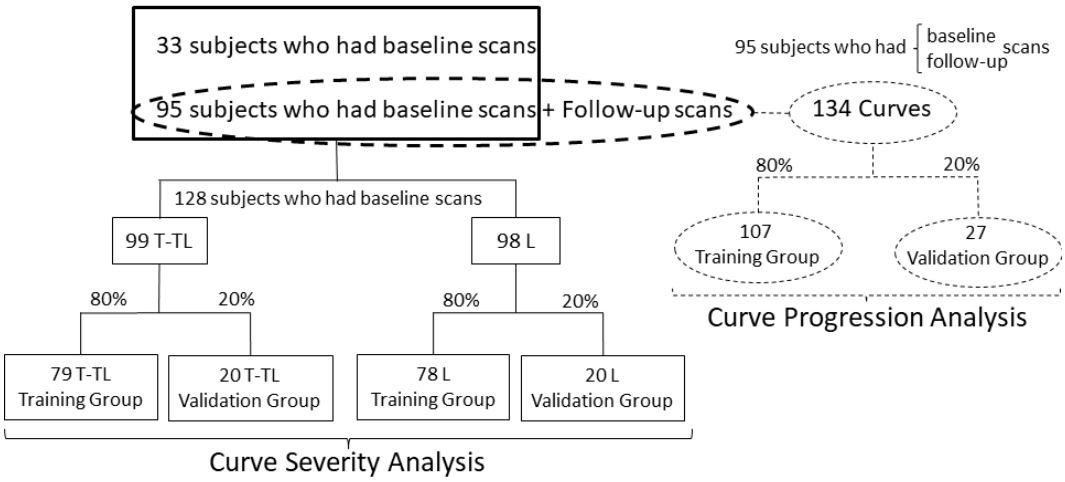

Figure 2-1- The number and location of curves used in the curve severity and curve progression analyses

2.3.2Asymmetry Analysis

The ST and radiograph scans were taken on the same day for each patient. The ST data was collected as described previously [3]. Briefly, four VIVID 910 3D laser scanners (KONICA MINOLTA Sensing Inc.) scanned the geometry of the patient's torso from each side, while the patient was positioned inside a custom designed frame with the torso in its natural posture. The accuracy of the scanning system was 1.8±0.9 mm [54]. The outputs of scanners were four binary files including the spatial locations (i.e., x, y, z coordinates) of the torso surface, and they were imported as inputs to the Geomagic Control software (3D System Corporation, CA, USA) to be merged for the whole torso. Unneeded parts of the scan, namely those for the frame, the head, pants, and arms, were cropped off to isolate the torso [3]. After smoothing the scanning noises, the asymmetry analysis was performed on the torso. The torso was duplicated and reflected along the sagittal plane. Then, the torso and its reflection were aligned by minimizing the sum of squares of distances between these two geometries[55]. The

misalignment between the torso and its reflection, resulting from the asymmetry shape of the torso, was measured using the 3D Comparison function and visualized using the contour plot in the Geomagic Control software. In our earlier study [3], the threshold between normal and abnormal deviations was set to 3.0 mm. However, in this study, the threshold, beyond which the asymmetry of the torso was considered scoliotic deformation, was varied from 3 mm to 10 mm with a 0.33 mm step until the isolated patches matched the curves observed in the radiographs by the clinicians in all subjects. The optimum cut point, which defined the minimum deviation as a scoliotic deformation and avoided patch overlap, was found to be 9.33 mm (Figure 2-2). This modification was applied only if the ST scan had a maximum deviation greater than 9.33 mm, otherwise the threshold of 3 mm was used as suggested by Komeili et al. [3, 22]. To measure the ST parameters, the scoliosis deformations were isolated from the other regions creating deformity patches. The macro, that was used by Komeili et al. [3], was modified to isolate the asymmetry patches from the other areas in the deviation contour map in Wolfram Mathematica (Wolfram Research, Inc., Mathematica 8.0.4.0). The process of isolating a deviation patch was as follows:

Step 1- Identify the point with the maximum deviation in the cloud of points and set it as the centre point of a sphere with a radius of 5 mm.

Step 2- Collect all points inside the sphere with the deviation greater than 9.33 mm (the optimum cut point) and include them in the isolated deviation patch.

Step 3- Consider each selected point as the centre of a new sphere.

Step 4- Repeat Step 2 and 3 to progressively expand the boundary of deviation patch.

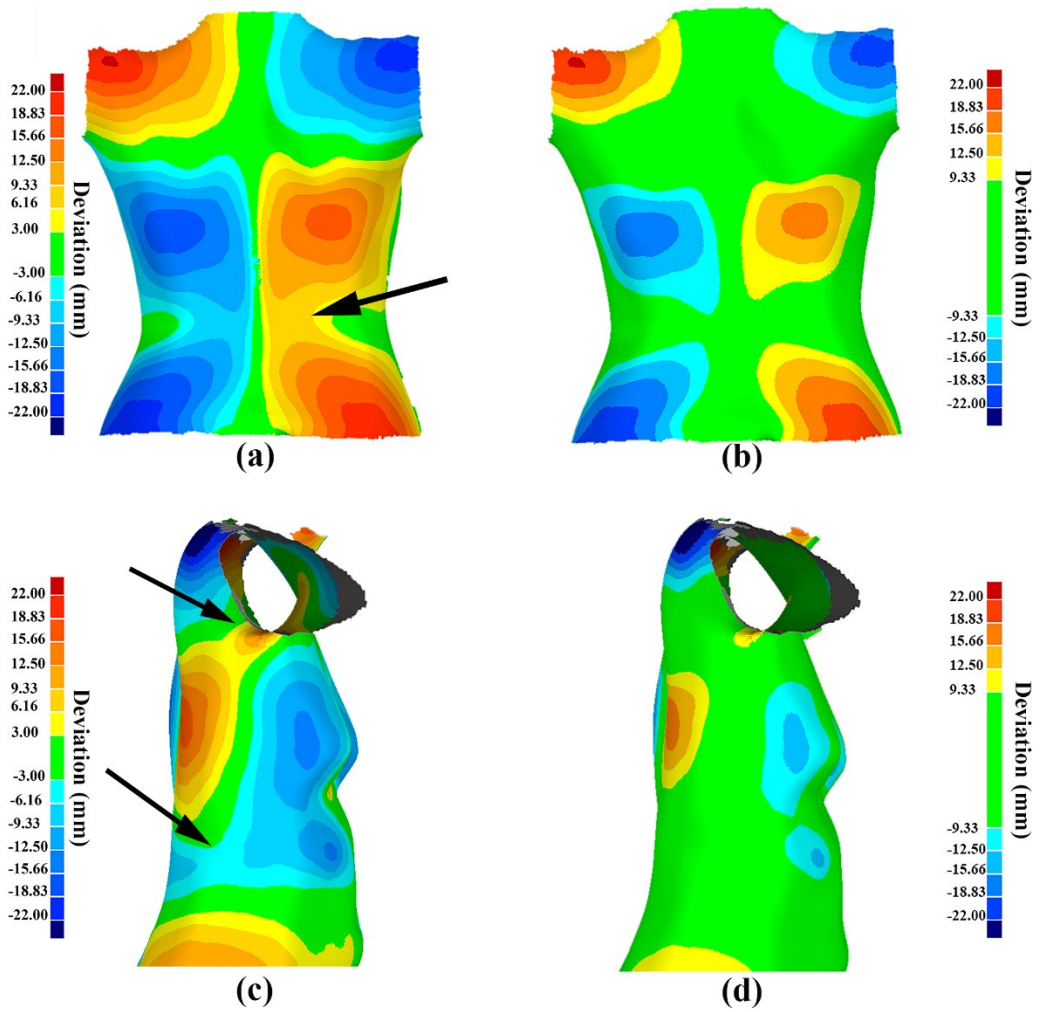

Figure 2-2- (a, c) the deviation patches of two torsos analyzed by Komeili et al. [3], in which the 3 mm deviation was defined as the threshold between normal and deformed area, and (b, d) the deviation patches of the same torsos analyzed by the modified ST analysis proposed in this study with the threshold of 9.33 mm. The arrows point to the artifacts in deviation patches, such as continuous deviation patches on the back and side of the torso and deviation patches due to the folded skin near the armpits, which were resolved after using the suggested modifications in this study. The green regions of the torso are considered normal. The blue and red patches represent abnormal protruded and indented regions of the torso, respectively, due to the scoliosis condition.

The maximum deviation (*MaxDev*) used in step 1 and the root mean square (*RMS*) of deviation patches were calculated, respectively, with the following equations:

$$MaxDev = Max\left(|Deviation_i|\right) \qquad i = 1, 2, 3, \dots, n \qquad \text{Eq. 1}$$

$$RMS = \sqrt{\frac{\sum_{i=1}^{n}(Deviation_i{}^2)}{n}} \qquad i = 1, 2, 3, \dots, n \qquad \text{Eq. 2}$$

where, *n* is the number of points representing the torso shape included in a given patch.

Figure 2-2 shows a contour-plot comparison between the deviation patches of a torso analyzed by Komeili et al. [3] (cut point 3.0 mm) and the deviation patches of the same torso analyzed by the modified ST analysis in this study (cut point 9.33 mm). In the contour plot shown in Figure 2-2-b, the green represents the area with deviation smaller than 9.33 mm, and shades of blue/red (referred to as deviation patches) indicate the area that protruded/sunken more than 9.33 mm, respectively. The patient's torso in an ST scan was divided into two parts, namely the lower one-third part was considered the lumbar area (L) and the upper two-third was considered the thoracic / thoraco-lumbar area (T-TL). The asymmetry parameters were assigned to each section, accordingly. The same procedure was repeated for the follow-up ST scans to calculate the progression of RMS and *MaxDev*, i.e. Δ*RMS* and Δ*MaxDev*. From the corresponding radiographs, progressions of Cobb angles (*ΔCA*) were retrieved from the clinical database. It was assumed that the direction of curve does not change from baseline to follow-up. During each patient clinic visit, Cobb angles are measured by the clinician and entered in the clinic database along with the end vertebra level and the apex for each curve.

Based on the Cobb angle, curve severity is classified into three groups in clinical practice: mild (10°≤ Cobb angle ≤25°), moderate (25°< Cobb angle ≤ 40°), and severe (40° < Cobb angle) [56]. An increase of 5 degrees or more in the Cobb angle during consecutive follow-up visits is recognized as a curve progression [12].

2.3.3 Classification Analysis

The classification tree technique implemented in IBM SPSS Statistics 24.0 was employed to build a classification model, using the asymmetry parameters (referred to as independent variables) to classify the curve severity (dependent variable i.e., Mild or Moderate/Severe). On purpose, the criteria in the development of classification tree used in this study placed more weight for the false negative error in the cost function of the classification tree analysis. The underlying rationale for this preference was to prevent classification of moderate or severe scoliosis curves in the mild group as much as possible, which could lead to a late diagnosis or an ineffective treatment of the scoliosis curve in the clinical application.

A separate tree was developed to classify progression (i.e., Progression or Non-progression) of the radiographic curve measurement (dependent variable). Note that the deviation patches in the T-TL and L sections were analyzed together to build the classification tree for categorizing the progression of torso asymmetry. The underlying motivation was the fact that, if a curve progression is identified by a classification system for a patient, a full vertebra radiograph scan is required regardless of its location and severity.

The classification analysis results were reported in Section 3, including the tabulated results to show the accuracy, sensitivity, and specificity [57]. In the curve severity classification, a positive test represents a moderate/severe curve and a negative test represents a mild severity. In the curve progression classification, a positive test represents the curve progression of 5 degrees or more and a negative test represents any curve progression less than 5 degrees (Non-progression).

The classification analysis mentioned above was conducted using the Training group such that the highest possible sensitivity was obtained, i.e. the false positive test was minimized. The obtained classification tree was used to classify the subjects in the Validation group. The resulting accuracy, sensitivity, and specificity of the

classification for the Training and Validation groups were compared to assess the validity of the method.

2.4 Results

2.4.1 Curve Severity Classification

None of patients were excluded from the analysis. Figure 2-3 and Figure 2-4 shows the severity classification trees for T-TL and L curves with the performance indices for the Training and Validation samples. Based on the statistical analysis, the *RMS* was a better independent variable (i.e., predictor) to be used in the classification of T-TL curves, i.e. deviation patches with *RMS* greater than 11 mm in T-TL section represented a moderate/severe curve regardless of its *MaxDev* value. While the combination of *RMS* and *MaxDev* worked well for identifying the severity of L curves; a deviation patch with *RMS* < 9.6 mm and *MaxDev* < 9.6 mm represented a Mild curve in L section, otherwise it represented a moderate/severe curve.

Out of 79 T-TL curves in the Training group, there were 35 curves with clinically moderate/severe curves, 34 of which were correctly identified with a sensitivity of 97%. Half of 44 mild curves were correctly classified in the mild group with a specificity of 50%. The majority of patients (22 out of 23), who were classified in the mild T-TL group based on their deviation patches, had truly a Cobb angle less than 25° in the corresponding radiographs, resulting in false negative error of only 3%. The overall accuracy of the T-TL curve severity classification was 71%. The classification of the 20 T-TL curves in the Validation group resulted in similar accuracy and sensitivity, with a maximum difference of ±7%, with respect to the Training group. No moderate/severe thoracic curves were misclassified by the ST analysis in the validation sample

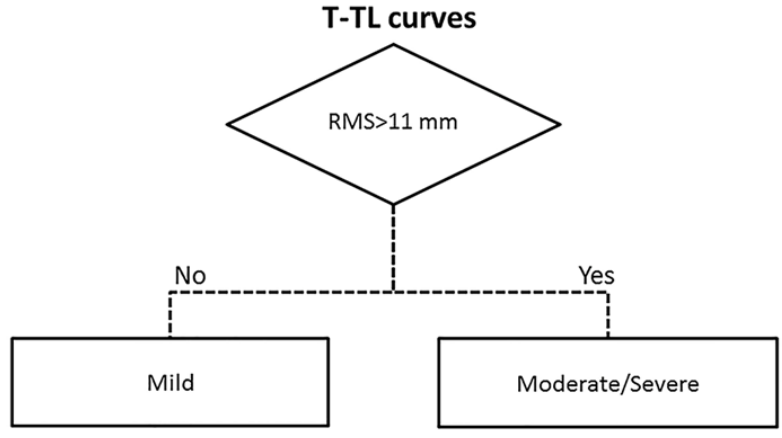

Training		RG (+)	RG (-)
ST	(+)	34	22
	(-)	1	22
ACC=71%		SE = 97%	SP = 50%

Validation		RG (+)	RG (-)
ST	(+)	9	7
	(-)	0	4
ACC=65%		SE = 100%	SP =36%

Figure 2-3- The classification trees and the tabulated accuracy (ACC), sensitivity (SE), and specificity (SP) values for the curve severity classification of T-TL curves. The (+) and (-) illustrate the moderate/severe and mild groups, respectively. RG: radiograph, ST: surface topography.

In the Training group of 78 deviation patches analyzed for the L section, 39 (50%) had moderate/severe curves based on the Cobb angle measurements in radiographs. The ST analysis successfully identified 35 of them in the moderate/severe group, resulting in a sensitivity of 90%. The mild L curves were correctly identified in 31% of cases but only 4 of 39 (11%) moderate/severe curves were missed by the ST analysis. The overall accuracy of the ST analysis in classifying curve severity in the L section was 60%. The classification of the 20 L curves in the Validation group also resulted in the same level of accuracy and sensitivity compared with the Training group. Only one (10%) moderate/severe lumbar curve in the Validation group was misclassified by ST as mild.

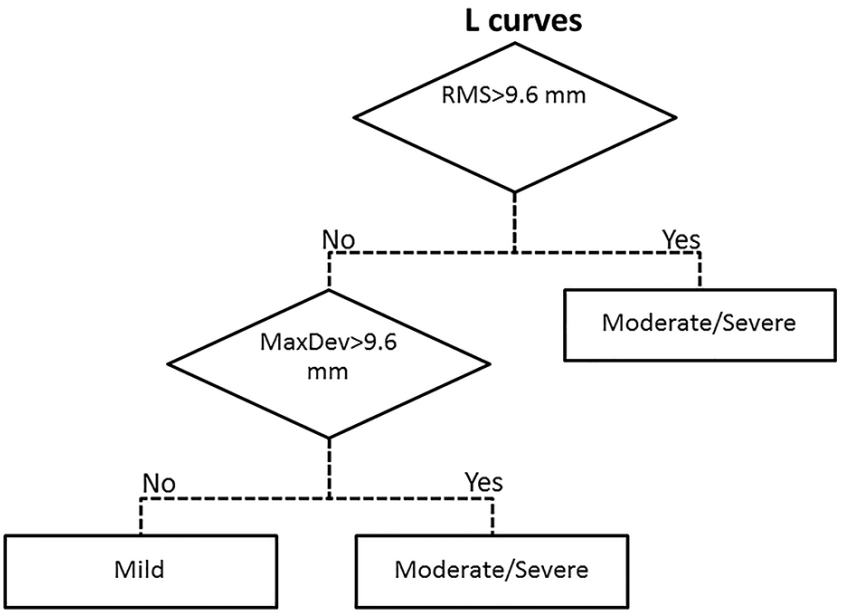

Training		RG (+)	RG (-)
ST	(+)	35	27
	(-)	4	12
ACC=60%		SE = 90%	SP = 31%

Validation		RG (+)	RG (-)
ST	(+)	9	7
	(-)	1	3
ACC=60%		SE = 90%	SP = 30%

Figure 2-4- The classification trees and the tabulated accuracy (ACC), sensitivity (SE), and specificity (SP) values for the curve severity classification of L curves. The (+) and (-) illustrate the moderate/severe and mild groups, respectively. RG: radiograph, ST: surface topography.

Figure 2-5 shows the distribution of the *RMS* and *MaxDev* of 79 T-TL and 78 L deviation patches and the thresholds for defining the severity of the curves in the Training group. The ST patches with *MaxDev* less than 9.33 mm were used in the Komeili et al. [3] classification tree to determine the severity of these deviation patches. Only one and four subjects with moderate/severe T-TL and L curves, respectively, were misclassified in the mild region, but their ST parameters were not far below the thresholds.

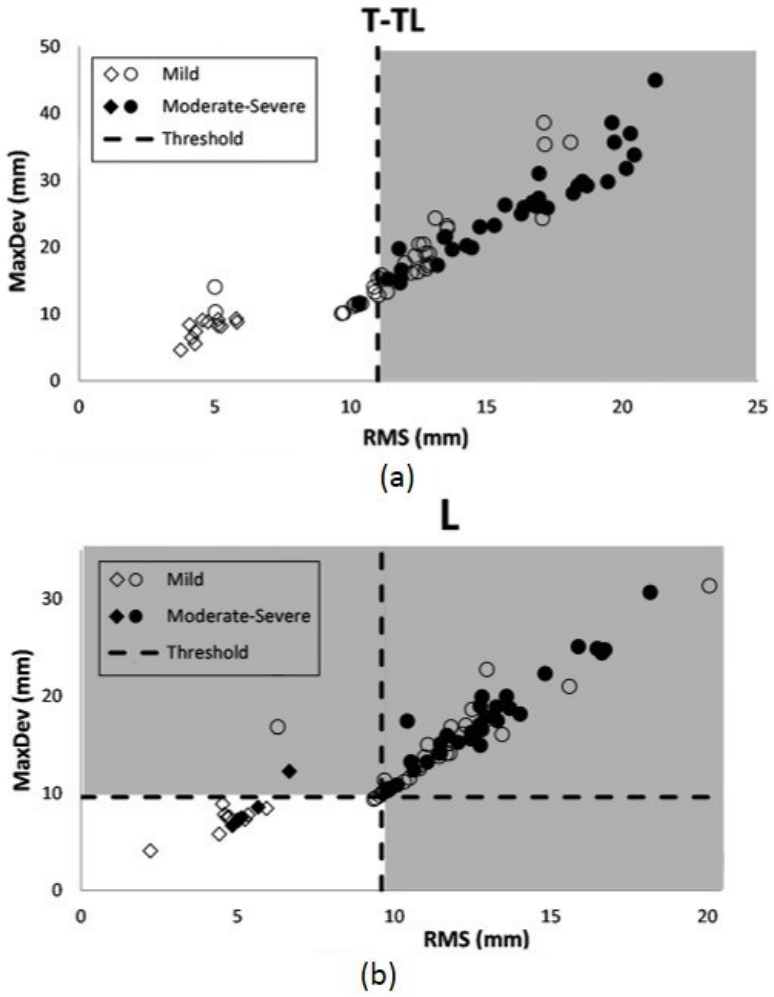

Figure 2-5- The distribution of *RMS* and *MaxDev* of (a) 79 T-TL, and (b) 78 L deviation patches and the thresholds for defining the severity of the curves. The shaded area shows the region corresponding to the Moderate/Severe classification. The open and closed symbols represent mild and moderate/severe curves based on the radiograph measurements, respectively. The ♦ and ◊ represent the deviation patches with *MaxDev* < 9.33 mm which were classified using the Komeili et al. [3] classification tree.

The performance of the modified ST analysis in identifying the curve severity proposed in this study was compared with our previous work [22, 25] in Figure 2-6-a. The sensitivity in the classification of curve severity was as high as the sensitivity in the work presented by Komeili et al. [26].

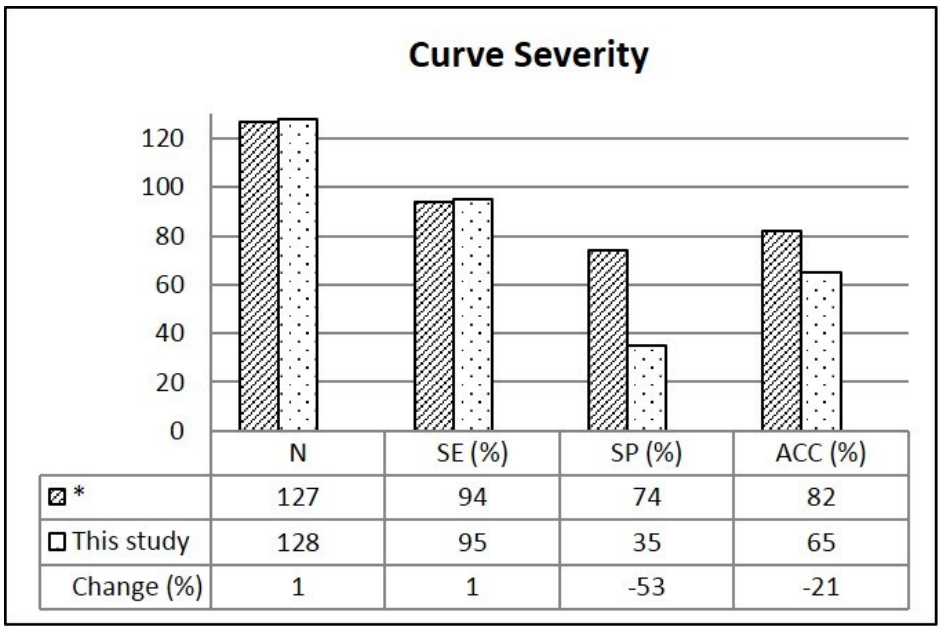

	N	SE (%)	SP (%)	ACC (%)
*	127	94	74	82
This study	128	95	35	65
Change (%)	1	1	-53	-21

(a)

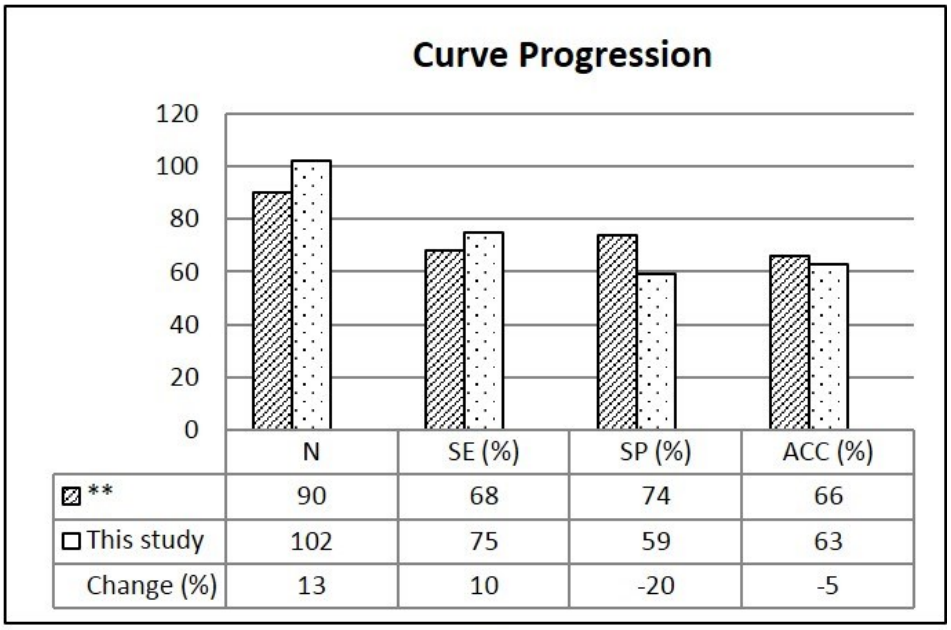

	N	SE (%)	SP (%)	ACC (%)
**	90	68	74	66
This study	102	75	59	63
Change (%)	13	10	-20	-5

(b)

Figure 2-6- Comparing the performance of the modified ST method in this study for all curves (T-TL and L curves in the Training group and Validation group) with previous studies in classifying the (a) severity and (b) progression of the scoliosis curves. (*):Komeili et al. [26], (**): Komeili et al. [29]

2.4.1 Curve Progression Classification

Figure 2-7 shows the classification tree for the classification of curve progression independent of the curve location, since the T-TL and L curves were mixed in the classification tree analysis. In the classification tree, a positive change of ST parameters between two consecutive visits correlated with more than 5 degrees curve progression. In other word, if a curve has positive *MaxDev* and *RMS* changes in the follow-up visit compared with the corresponding values in the baseline assessment, the curve is considered as progression and the patient needs radiography for further assessments.

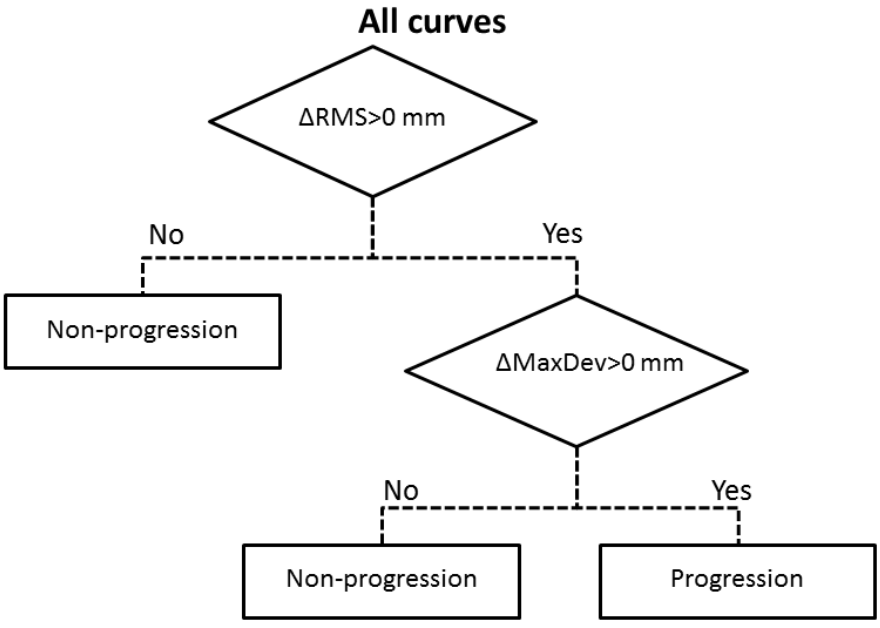

Training		RG (+)	RG (-)
ST	(+)	17	35
	(-)	5	50
ACC=63%		SE = 77%	SP = 59%

Validation		RG (+)	RG (-)
ST	(+)	4	8
	(-)	2	13
ACC=63%		SE = 67%	SP = 62%

Figure 2-7- The classification tree for categorizing patients in Progression and Non-progression groups using the Δ*RMS* and Δ*MaxDev* parameters. The (+) and (-) in the tables represent the Progression and Non-progression groups, respectively. ACC: accuracy, SE: sensitivity, SP: specificity, RG: radiograph, ST: surface topography.

Out of 107 curves in the Training group, 22 curves increased at least by 5 degrees, while there were no clinically important progressions for the other 85 curves. Based on the analysis, 17 out of 22 curves were accurately identified in the progression group (i.e., sensitivity 77%). Five (22%) of the cases with curve progression were missed. The percentage of the non-progressive curves that were detected by the asymmetry analysis was 59%. The diagnostic accuracy was 63%. The classification of deviation patches in the Validation group also resulted in an accuracy of 63% with a sensitivity of 67%, which are close to the corresponding values for the Training group. Figure 2-8 illustrates the variation of ST parameters in 107 deviation patches analyzed in baseline and follow-up visits, and the thresholds for identifying the scoliosis curves having progressed. There were 4 patients for whom both ST parameters improved, however their scoliosis curves progressed.

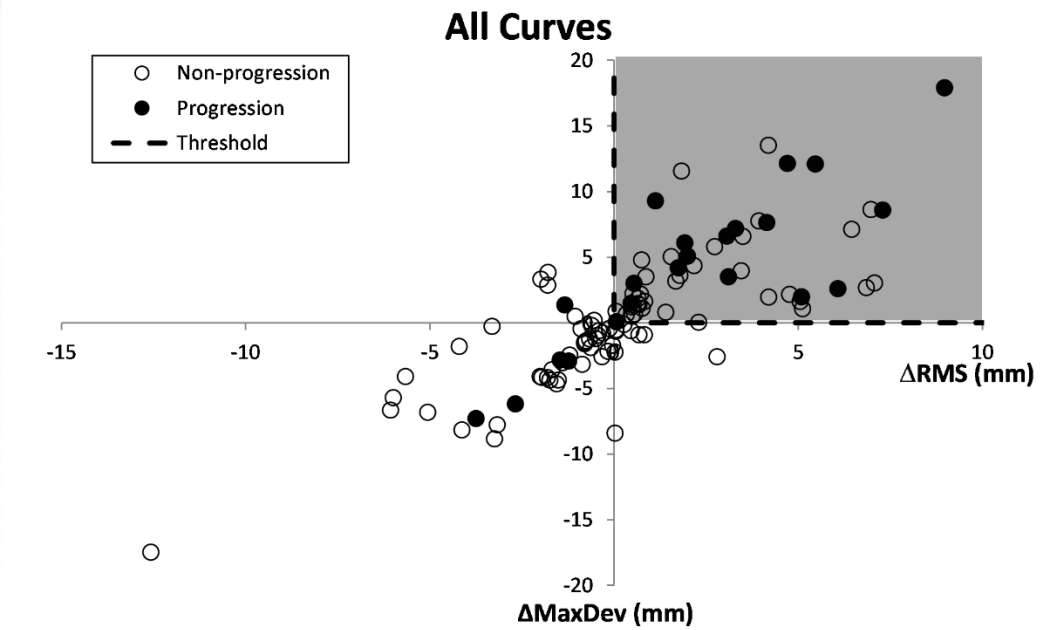

Figure 2-8- The distribution of Δ*RMS* and Δ*MaxDev* parameters. The threshold of Δ*RMS* and Δ*MaxDev* are shown with the dashed lines. The shaded area shows the region that is considered as the Progression group. The close and open circles represent a progressed (ΔCA ≥ 5 degrees) and Non-progressed (Δ*CA* < 5 degrees) case based on the radiograph measurements, respectively.

Compared with the sensitivity and accuracy obtained in Komeili et al. [29] study, the sensitivity of the ST method in monitoring curve progression in this study was improved by 10.3% (i.e., from 68% to 75%), while accuracy decreased by a relatively small percentage, 4.5%, (i.e., from 66% obtained in Komeili et al. [29] to 63%) (see Figure 2-6-b).

2.5 Discussion

The markerless asymmetry analysis developed previously [3] showed promising results in identifying curves with progression in the follow-up visits with the potential ability of reducing 43% of radiation exposure in the monitoring of AIS. The research presented in this study aimed at modifying the markerless asymmetry analysis by simplifying the application of the previously developed method while also improving the sensitivity and accuracy of the classification in identifying the moderate/severe curves and the progression of the scoliosis curve. While the need for manual handling of deviation patches was resolved and the sensitivity in identifying the progressed curves improved by 10%, the overall accuracy of the method decreased by 5%. As a result, the applied modifications on the original method resulted in more conservative monitoring and curve severity assessment of scoliosis where fewer cases of moderate/severe curves and progression cases were missed (see Figure 2-6).

In this study, the optimum threshold of deviation for isolating the deviation patches was found to be 9.33 mm. The isolated deviation patches were generally smaller in size than those obtained in Komeili et al. [3, 22] (see Figure 2-2). The modified code successfully prevented the extensions of isolated deviation patch to the anterior section of the torso and around the armpits, and clearly separated the boundaries between the deviation patches in ST scans of patients with a double or triple scoliosis curves shown in Figure 2-2. Moreover, we expect that the reliability of the method in repeating the analysis would increase by automating the patch isolation step and avoiding human intervention in the ST analysis process.

The accuracy of 65% and 60% were obtained in categorizing the severity of T-TL and L curves in the Validation cohort, respectively as show in Figure 2-3 and Figure 2-4. This level of accuracy was approximately the same as the accuracy obtained for the Training group, indicating repeatability of the classification model in the classification of T-TL curves severity.

The distribution of *MaxDev* and *RMS* parameters of subjects in Training group in Figure 2-5 illustrated that the correlation of ST parameters with the curve severity in T-TL region was better than in the L region. In T-TL curves, all ST scans with *MaxDev* less than 9.33 mm in Figure 2-5, which were denoted by ◊ or ♦, had *Cobb angle* less than 15 degrees and were correctly classified using the original method developed by Komeili et al. [3].

The monitoring of T-TL and L curves progression were analyzed separately (results are not shown) and no difference in the sensitivity, specificity, and accuracy was obtained if T-TL and L curves were analyzed in one group. Therefore, for the monitoring of scoliosis curve T-TL and L curves were mixed and analyzed using only one classification tree which is likely more practical clinically (Figure 2-7). The variation of ST parameters in this study was correlated with the progression of Cobb angle measured in radiographs with a sensitivity of 67% for the Validation group in Figure 2-6. However, some negative changes in *ΔRMS* and *ΔMaxDev* were obtained for patients with a positive Δ*CA* in Figure 2-7. The proposed threshold of 9.33 mm for isolating the deviation patches in this study resulted in smaller accuracy and sensitivity in monitoring curve progression specifically for patients with mild and moderate curves in the baseline. Excluding area with the deviation less than 9.33 mm from the deviation patches provided less information about the torso shape for monitoring the deformities over time. Therefore, any change in the areas with the deviation less than 9.33 mm over time was not included in the analysis, which led to the misclassification of multiple curves especially in the patients with moderate scoliosis curves, where relatively small portion of torso had deviations greater than 9.33 mm (see Figure 2-8). Our results showed that curve progression monitoring appears to be 100% (4/4) accurate for patients with severe scoliosis curve in baseline who progressed in the follow-up scans

(tabulated results are not shown). Therefore, monitoring mild and moderate scoliosis curves that present smaller asymmetry on the torso surface with respect to the severe curves, using the modified asymmetry analysis method in this study involves a higher risk of false negative. The case-by-case investigation of patients who were incorrectly identified in the Progression group (false positive) showed that 55% of the population had truly a larger Cobb angle in the follow-up radiographs compared to the baseline. However, the positive increase of Cobb angle was not significant enough to be considered as a progression, i.e., ΔCA in the range of 0–5 degrees. Although a follow-up radiograph is not necessary for this group of patients, considering the error in Cobb angle measurements and the small degree of progression in many of the participants might sufficiently justify taking a radiograph in the follow-up.

The overall sensitivities in identifying curve severity in this study were similar to the corresponding values in Komeili et al. [26], 95% and 94%, respectively (Figure 2-6). The reduction in the overall accuracy (i.e. 82% to 65%) in identifying the severity of the curve using ST parameters in this study with respect to Komeili et al. [26] was caused by a larger false positive error rather than false negative error, i.e. classifying a considerable number of the deviation patches of patients with mild scoliosis curves in the moderate/severe group. One third of the misclassified mild curves had a *Cobb angle* in the range of 20–25 degrees, which is on the margin of the mild/moderate severity definition used in the scoliosis clinic. It should be noted that, there is a ±5 degrees inter- and intra-observer error in the measurements of Cobb angle [44, 45], therefore there is a possibility that some of the misclassified mild curves with Cobb angle in the range of 20-25 degrees could have been diagnosed as moderate if the radiograph assessment had been repeated.

The overall sensitivity of 95% in Figure 2-6 indicates a high ability to detect moderate/severe curves which are more susceptible to progress than mild curves and thus do require further attention. Taking full torso radiograph in the follow-up visits is the standard for all patients at the scoliosis clinics, hence, subjects whose classification was false positive would not get more radiographs than others without ST assessment, and we would still prevent radiograph exposure for some truly negative cases. Komeili et al. [29] reported a classified 43% reduction in the radiograph acquisition if they

combined the ST analysis with the radiograph assessment in the monitoring of curve progression. Because of the slightly lower accuracy observed in this study in screening for curve progression, we estimate a 5% lower reduction of the need for radiograph compared with the work of Komeili et al. [29]. Nevertheless, the asymmetry analysis improvements suggested in this study would result to a more conservative monitoring. Because of the higher sensitivity obtained (Figure 2-8-b) a lower number of patients would suffer from missing the opportunity of an early diagnosis of curve progression by using our improved ST analysis.

We had enough data for statistical analyses, however we have to acknowledge that only 39 patients in the Training group had curve progression, which may not represent the diversity of scoliosis curve types, such as single and double curves. Another limitation of our study is exclusion of trunk axial rotation in our classifications, which is an important piece of information for clinicians in prescribing patient specific braces. It may be possible to improve the accuracy of curve progression diagnosis if more ST parameters, such as curvature of back valley [60] and trunk rotation [61], were combined with the *RMS* and *MaxDev* parameters included in this study. The strong correlation between deviation patches and spinal curve location can also provide good information about the kyphosis and lordosis angles obtained from radiographs, which, however, may not be necessary if the proposed method is used only in scoliosis cases clinics. Our asymmetry analysis is compatible with the ST database of those clinics that do not use the same acquisition system in capturing the full torso geometry as we do. The markerless feature of the asymmetry analysis reduced the common limitations of ST methods, such as dependency of the method to specific local marker-based measurements, and data acquisition technique. Having the 3D geometry of the torso, in normal posture, is the only required condition for using this method. Our strategy in classifying curve severity and curve progression could also be followed in other ST classification systems, in which the cosmetic parameters of the torso are correlated to the scoliosis curve characteristics. Our conservative approach in minimizing the number of false progression and false moderate/severe in the classification system may result in a lower overall accuracy, however it would

reduce the risk of missing a progressed or moderate/severe curve, which is the main concern in replacing radiographs with ST assessments in scoliosis clinics.

2.6 Conclusion

The modified thresholds used to define asymmetry patches successfully separated the deviation patches in the upper two-third (T-TL) section from the lower one-third part (L) section and eliminated the manual work, which was previously necessary for isolating the deviation patches in some patients. The modified thresholds used in this study, allow automation of the analysis and led to the same level of sensitivity in identifying the curve severity as in our previous work. Similarly, the modified analysis led to similar sensitivity for monitoring the progression of the scoliosis curve as our previous work. Despite the novel method being unfortunately associated with a higher risk of misclassification of cases with no progression significant numbers of patients (approximately 39%) may be able to avoid radiographs confident that their curves did not progress.

3

Customized k-Nearest Neighbourhood Analysis in the Management of Adolescent Idiopathic Scoliosis Using 3D Markerless Asymmetry Analysis[1]

3.1 Abstract

Adolescent Idiopathic Scoliosis (AIS) is a 3D spinal deformity characterized by curvature and rotation of the spine. Markerless surface topography (ST) analysis has been proposed for diagnosing and monitoring AIS to reduce the X-ray radiation exposure to patients. A total of 128 AIS patients with baseline and follow-up radiograph and ST assessments were recruited. This method captures scans of the cosmetic

[1] This chapter has been submitted to Journal of Computer Methods in Biomechanics and Biomedical Engineering. Maliheh Ghaneei, Ronald Ekyalimpa, Lindsey Westover, Eric Parent, Samer Adeeb, "Customized k-Nearest Neighbourhood Analysis in the Management of Adolescent Idiopathic Scoliosis Using 3D Markerless Asymmetry Analysis."

deformity of the torso using visible, radiation-free light. The asymmetry analysis of the torso, represented as a deviation contour map with deviation patches outlining the areas of cosmetic asymmetries, has previously been shown to classify the severity and progression of the condition in comparison with radiographs, by using classification trees. While the classification results were promising, it was reported that some mild curves were erroneously diagnosed. Furthermore, this approach is highly sensitive to threshold values selected in the decision trees. Therefore, this study aims to define a custom k Nearest Neighbourhood Classifier algorithm for AIS classification to improve the accuracy, sensitivity, and specificity of classifying curve severity and curve progression in AIS. This method is one of the common and simple machine learning algorithms where input parameters are used to determine the k closest stored data points and then map them to an output through a systematic classification or a regression process,

Curve severity was classified with 80% accuracy (sensitivity = 81%; specificity = 79%) for thoracic-thoracolumbar curves and 72% (sensitivity = 93%; specificity=53%) for lumbar curves. This represents an improvement over the previous method with curve severity accuracies of 77% and 63% for thoracic-thoracolumbar and lumbar curves, respectively. Additionally, curve progression was classified with 93% accuracy (sensitivity=83%; specificity=95%) representing a substantial improvement over the previous method with an accuracy of 59%. The current method has shown the potential to further reduce radiation exposure for AIS patients by replacing X-rays for mild and non-progressive curves with ST analysis.

Keywords: Scoliosis, Adolescent Idiopathic Scoliosis (AIS), surface topography, 3D markerless asymmetry analysis, monitoring, curve progression, k-Nearest Neighbour

3.2 Introduction

Spinal deformity is associated with cosmetic abnormality, difficulty in health-related quality of life, and can result in impairment such as difficulty breathing in the most severe cases [2, 18]. Adolescent idiopathic scoliosis (AIS) is a frequent form of such deformity [41] which requires repetitive monitoring using X-rays [42]. The Cobb angle is measured on radiographs to document the location and the severity of curves [43]. This approach has two primary limitations: first, X-ray radiation has harmful effects, including an increased risk of cancer for this adolescent population [37, 38] and second, the Cobb angle is a two-dimensional measurement of a three-dimensional deformity [32, 51].To overcome these limitations, our team developed a markerless surface topography (ST) technique with the purpose of evaluating the whole surface of the patient's torso using a 3D laser scanner. The proposed ST monitoring strategy suggests that patients presenting with either mild (Cobb angle $< 25^{\circ}$) or non-progressive (ΔCobb angle (ΔCA) $< 5^{\circ}$ increase) curves could avoid an X-ray since the typical standard of care for these patients involves only observation or no change in treatment, respectively. The ST analysis technique presented in our previous work showed the potential to eliminate X-rays for some patients [3].

The cosmetic deformity associated with AIS involves torso asymmetry. A person with no spinal curvature is approximately symmetric across the midsagittal plane, which means that the person's torso and its reflection along this plane are almost perfectly aligned [63]. However, for a person with an asymmetric torso, the sagittal plane is no longer a plane of symmetry. Our method takes advantage of the best plane of symmetry identification method introduced by Hill et al. [55] to assess the deformity of the scoliotic spine. The best plane of symmetry is roughly aligned with the midsagittal plane; however, the actual plane is determined by minimizing the sum of distances between the patient's torso and its bilateral reflection [3]. The asymmetry is then illustrated using a deviation contour map plotted on the patient's torso. The effects of the spinal curvature are visualized in terms of dense colour areas called deviation patches containing many points whose colours represent the distance between the original and reflected torsos, depicting both areas of protrusion or depression relative

to the other side [3]. The maximum and root mean square of these deviations are computed as asymmetry parameters (*MaxDev* and *RMS*, respectively). These asymmetry parameters have been compared with the Cobb angle measured in the corresponding region of the torso to create decision trees classifying curve severity on a given test day and progression between consecutive examinations [3, 28, 54].

Decision trees were used to classify the curve severity (mild or moderate/severe) and to evaluate clinically significant progression of the curves ($\Delta CA \geq 5^{\circ}$) through one time interval [29]. The results were promising for curve severity classification especially in detecting moderate/sever patients (Cobb angle $\geq 25^{\circ}$; sensitivity = 95%, specificity = 35%) [64]. However, the previous work had several limitations. Some mild curves were erroneously diagnosed indicating that the method showed high sensitivity and low specificity. Furthermore, the decision tree analysis is oversensitive to threshold values selected. In other words, a minor change in one variable leads to major changes in subtree below or even may destabilize the tree [65]. Threshold values can be controlled to achieve the highest possible sensitivity to moderate/severe cases, which however may reduce the specificity by identifying mild patients as moderate/severe. The other significant drawback of the decision tree analysis is that in defining the classification trees it was assumed that as the asymmetry parameters increase, the Cobb angle also increases. However, it will be shown in this study that as the RMS increases, the *MaxDev* increases while the Cobb angle fluctuates within a wide range. Consequently, this assumption may result in the misclassification of the patient status.

To overcome the limitations of decision tree analysis, an appropriate classification model is sought to relate the ST parameters and the Cobb angle, which in general exhibit lack of correlation. The first classification rule was proposed by Fisher in 1936 in statistical classification literature, after which other classification models were proposed and applied [30]. The k-nearest neighbour (*k-NN*) algorithm is one of the simplest machine learning algorithms where input parameters from a certain number (k) of the closest data points within a Training Group are mapped them to an output through a systematic classification or a regression process [37]. The output of

the classification is a class generated from the k-neighbours.[66] The current study aims to use the k-NN method for classifying patients with AIS on the basis of their ST asymmetry parameters in terms of curve severity and curve progression to reduce the errors of such classification efforts observed when using decision trees [64].

3.3 Materials and Methods

3.3.1 Data Collection

ST scans and X-ray radiographs of 128 AIS patients recruited from the scoliosis clinic were used in this study. Patients included in the study had an age range of 10 to 18 years (14.4±1.8 years) with a mean Cobb angle of 26.5° (from 10° to 46°). 100 patients (78%) were female and 28 (22%) were male. Follow-up scans of 95 patients were available in a 1 year ± 3 month interval. Both baseline and follow-up data were used in the curve severity analysis, which resulted in 176 thoracic / thoraco-lumbar (T-TL) curves and 167 lumbar (L) curves, including patients with multiple curves. To monitor curve progression from baseline to follow-up, 95 ST and radiograph pairs with a total of 134 curves were used.

The raw ST data was obtained by a standard scanning procedure. Images were acquired from the front, back, left and right of the patients with four VIVID 910 laser scanners (KONICA MINOLTA Sensing Inc.) in the clinic on the same day as their radiographs [3]. After merging the ST data to create the full 3D model of the patient in Geomagic Control (3D System Corporation, CA, USA), the torso was isolated by cropping the frame and unnecessary parts such as the lower extremities, head, and arms [3]. The full 3D torso was duplicated and mirrored along the sagittal plane. Then the original torso and its reflection were aligned such that the deviations between corresponding points were minimized. The misalignment between the two torsos was visualized in the deviation contour map plotted on the torso [3]. The threshold between normal and abnormal deviations was 9.33 mm if the ST scan had a maximum deviation

greater than 9.33 mm [64], otherwise the threshold of 3 mm was used as suggested by Komeili et al. [3, 25] (see Figure 3-1).

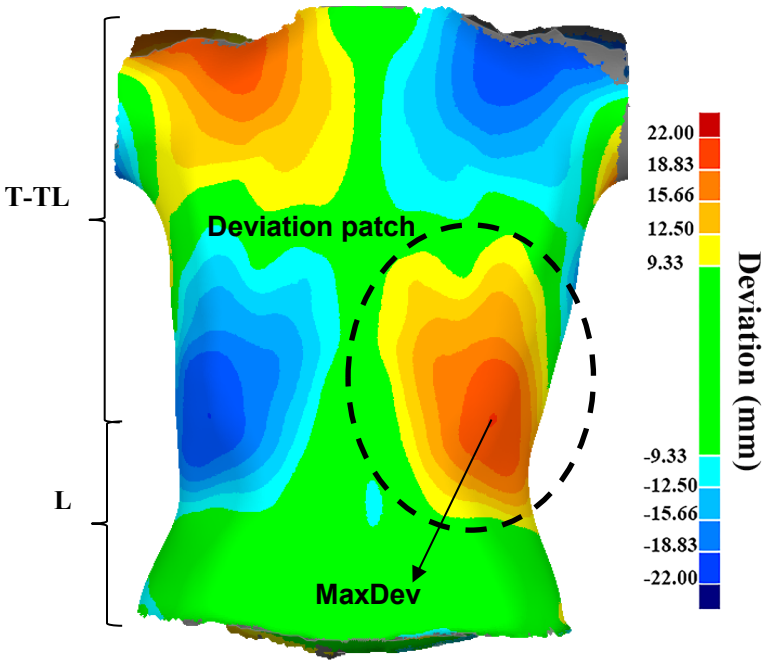

Figure 3-1- Deviation contour map

Blue areas indicate that the original torso is outside of the reflected torso, i.e. original torso covers the reflected torso, and red areas indicate that the original torso is inside of the reflected torso. The shades of blue and red (deviation patches) illustrate the areas of deviations corresponding to the level of the existing scoliosis curves. The maximum absolute distance between the original torso and its reflection was recorded as the *MaxDev* and the root mean square of all the deviations within each patch was recorded as the RMS according to the following equations:

$$MaxDev = Max\ (|Deviation_i|) \qquad i = 1, 2, 3, \dots, n \qquad \text{Eq. 1}$$

$$RMS = \sqrt{\frac{\sum_{i=1}^{n}(Deviation_i{}^2)}{n}} \qquad i = 1, 2, 3, \dots, n \qquad \text{Eq. 2}$$

where, n is the number of points within the deviation patch under analysis. The ST scan of a patient's torso was divided into two parts. The lower one-third part of the

torso was considered the (L) area and the upper two-thirds was considered the (T-TL) area. The asymmetry parameters were classified as L or T-TL according to the location of the asymmetry patch from which they were extracted. To study the curve progression of those patients who had ST data at a follow-up visit, the differences of the *MaxDev* and *RMS* from baseline to follow-up were computed, i.e. *ΔRMS* and *ΔMaxDev*, and It was assumed that the direction of curve does not change from baseline to follow-up.

3.3.2 Data Analysis

3.3.2.1 Preliminary data analysis

Preliminary studies on data were performed by plotting charts for asymmetry parameters and Cobb angle across the curve IDs (see Figure 3-5). The correlation between parameters was examined through linear trend lines plotted on the charts along with corresponding coefficients of determination (R^2)

$$R^2 = 1 - \frac{\sum_{i=1}^{n}(y_i - f_i)^2}{\sum_{i=1}^{n}(y_i - \bar{y})^2} \qquad n = 1,2,3,\dots,n \qquad \text{Eq. 3}$$

Where $\bar{y}_i = \frac{1}{n}\sum_{i=1}^{n} y_i$ is the mean of observed data and f_i is the corresponding point at the fitted trend line.

3.3.2.2 Classification algorithms

Traditional neighbourhood classifier: The traditional neighbourhood classification method [37] will be introduced, in general. This method consists of two phases, namely training and classification. In the training phase, all the features (independent and dependent parameters) of the existing data points are stored in a group, called the Training group. Next, in the classification phase, a new data point can be categorized based on the most frequent dependent variable in the Training group who has the smallest difference with the independent variables.

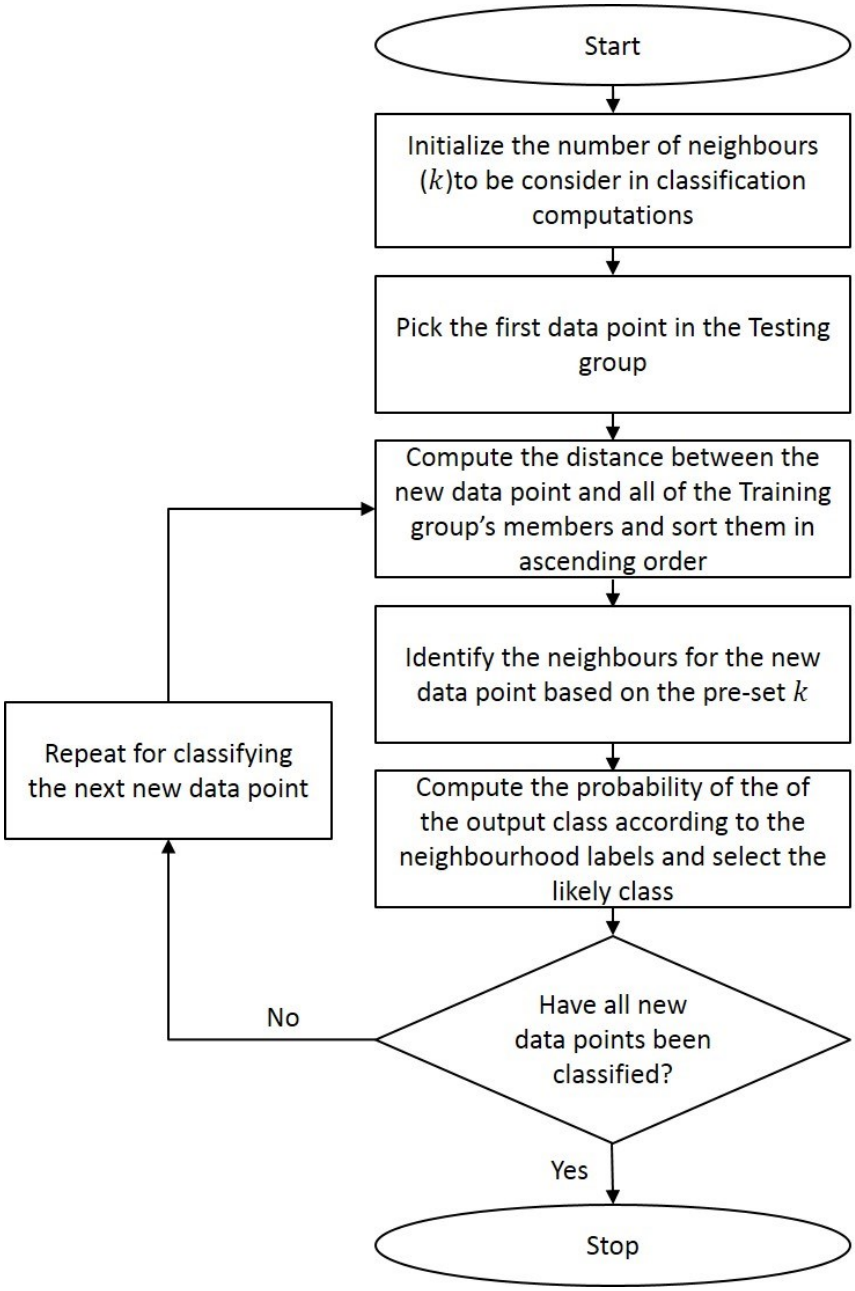

Figure 3-2- A Flowchart summarizing the traditional k-NN classification algorithm

To calculate this difference, Euclidean Distances (Eq. 4) between the new data point and all of the Training group's members are first computed using the values for each independent variable. Then, the data points within the Training set are ranked in ascending order based on their respective distances. Next, the first k numbers of

ranked data points are collected as neighbours of the new data point to subsequently determine the probability of the output class according to the neighbourhood labels. (Figure 3-2)

$$d_{Euclidean} = \sqrt{(x_1 - y_1)^2 + (x_2 - y_2)^2 + \cdots + (x_n - y_n)^2} \quad \text{Eq. 4}$$

Custom neighbourhood classifier: A custom neighbourhood classifier is defined in this study to enhance the classification results such that each of the independent variables (e.g. *RMS* and *MaxDev*) are used in sequential order starting with the one that has the strongest correlation with the output class (e.g. curve severity) and ends with that which has the weakest correlation. In other words, the set of first neighbours in the first round is used as a Training group to be evaluated for the neighbours in the next iteration. This process was repeated until all independent variables (e.g. two independent variables in this study) were evaluated. The selection of neighbours based on a specific independent variabler is achieved by calculating the absolute difference between the data point under study to the points in the dataset from which neighbours are to be selected. The rest of the classification phase was the same as what has been described in the traditional neighbourhood classification section. It should be noted that the value for the number of neighbours in the final classification phase is kept odd to facilitate identification of the output class associated with the data point under study.

3.2.2.3 Training classifier models and classification model performance evaluation

In this study, the data points are contour patches associated with individual curves and were randomly divided into two groups, namely the Training group and the Testing group using common data splitting rules (80:20).

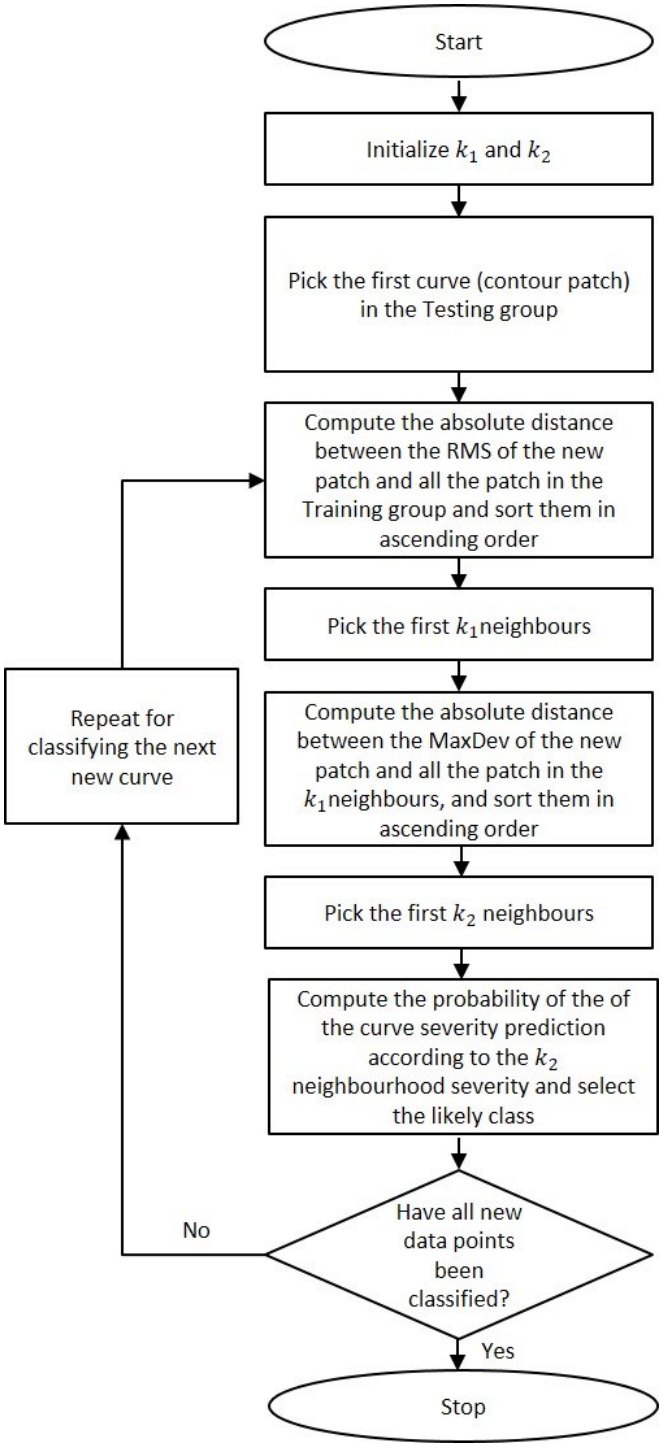

Figure 3-3- Flowchart of the customized k-NN classification algorithm for curve severity classification

For the curve severity classification two independent parameters, *RMS* and *MaxDev*, are used. Hence, only two neighbourhood computation iterations are required. The number of neighbours in the first and second iterations are denoted as k_1 and k_2, respectively. The classification phase starts with *RMS* rather than *MaxDev* since it has illustrated stronger correlation with the curve severity based on the preliminary analysis in this study as well as in the work of Ghaneei et al. [64]. The output class is the curve severity classification (either mild or moderate/severe). The process described is summarized in the flowchart presented in Figure 3-3. Wolfram Mathematica (Wolfram Research, Inc., Mathematica 8.0.4.0) was used to automate this process.

For curve progression, Δ*RMS* and Δ*MaxDev* are the independent variables used in the first and second classification phases, respectively, and the output class is the progression status (either progression or non-progression).

The performance of the models developed for classifications were assessed based on sensitivity, specificity, and total accuracy. For curve severity, a positive result represents a moderate/severe curve and a negative result shows mild severity. For curve progression, a positive result indicates a progressive curve (increase in Cobb angle$\geq$5° over the time interval) and a negative result is a non-progressive curve ($<$5°). The analysis was conducted based on maximizing the sensitivity and minimizing the false positive test. The classified results were based on the ST analysis and the actual results were based on the radiographic measures. Table 1 presents a matrix that was used to determine the performance measures and parameters used in the classification process.

Table 3-1- Calculation of the accuracy, sensitivity and specificity

		Radiograph	
		$+$	$-$
Surface Topography	$+$	True positive (TP)	False positive (FP)
	$-$	False negative (FN)	True negative (TN)
Accuracy $(\mathrm{TP}+\mathrm{TN})/(\mathrm{TP}+\mathrm{FN}+\mathrm{FP}+\mathrm{TN})$		Sensitivity $\mathrm{TP}/(\mathrm{TP}+\mathrm{FN})$	Specificity $\mathrm{TN}/(\mathrm{FP}+\mathrm{TN})$

3.2.2.4 Parametric studies for the customized k−NN classification

The accuracy of the results from the customized k-NN class are dependent on the number of neighbours (k) selected for each neighbourhood [67]. As such, a parametric study was performed to establish the appropriate number of neighbours that generates the best results. k_1 and k_2 were each varied sequentially from 1 to 20 and the optimal values were those that provided the best results (sensitivity, specificity, and accuracy).

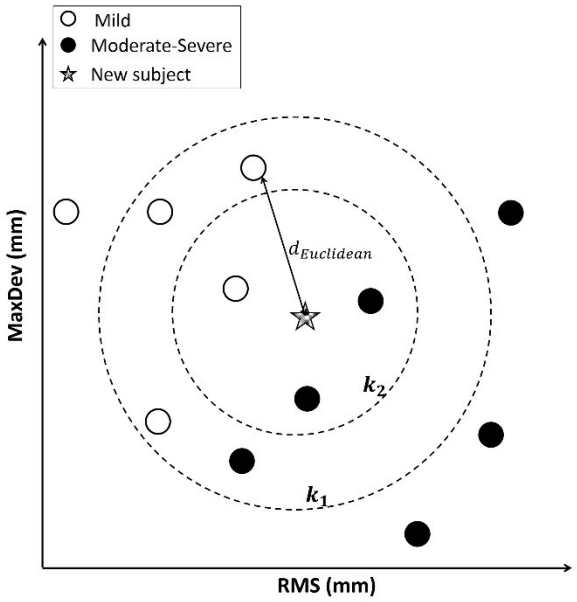

Figure 3-4- Simplified sketch of the customized k-NN algorithm

3.4 Results

3.4.1 Curve severity classification

For L curve, in Figure 3-5-a, the curve parameters *RMS*, *MaxDev*, and Cobb angle were plotted against the curve ID, where the curve IDs were ordered by increasing RMS. While in Figure 3-5-b, the asymmetry parameters were plotted against the Cobb angle.

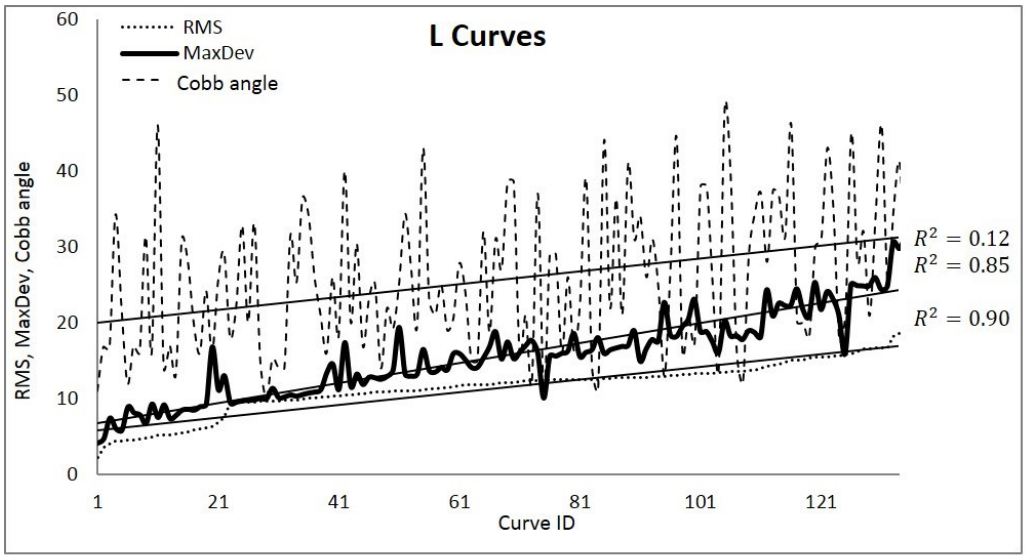

(a)

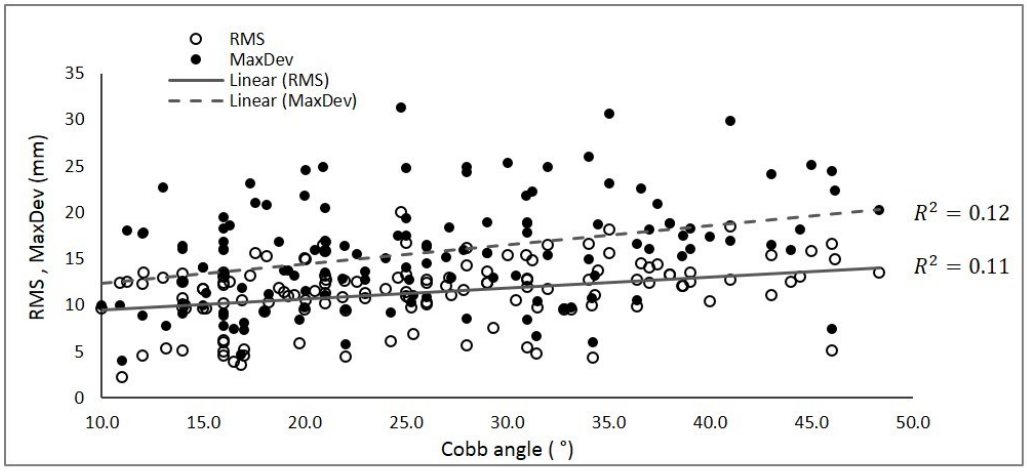

(b)

Figure 3-5- Comparing the associations between RMS, MaxDev and Cobb angle

Figure 3-5-a reveals that while *RMS* and *MaxDev* are closely related to each other, the Cobb angle does not follow the same trend and fluctuates within a wide range. *RMS* and *MaxDev* vary linearly with curve ID with R^2 values of 0.90 and 0.85, respectively. Conversely, the corresponding Cobb angles vary widely with curve ID and do not follow a linear trend (R^2=0.12). More clearly, Figure 3-5-b demonstrates that with the assumption of linear trend between asymmetry parameters (RMS and MaxDev) and Cobb angle, R^2 values are almost 0.1 which shows no linear relations exist.

There were a total of 176 T-TL curves and 20% of them (35 curves) were randomly selected to establish the Testing group while the rest (141 curves) were considered as the Training group. The ultimate goal of the proposed method is the proper detection of moderate/severe patients, which is equivalent to achieving the highest sensitivity. With this goal in mind, the optimum values for neighbours in the first and second iterations were found to be 3 for both (k_1 =k_2=3). Thus, it is only needed to consider the first three ranked data points from the Training group and the severity of the patient under study is decided based on the most frequent class labels (mild or moderate/severe) among such ranked data.

Of the 35 T-TL curves in the Testing group, 16 were moderate/severe and 19 were mild based on radiographic measures. Table 2 illustrates the curve severity classification for the curves in the Testing group. As it can be seen the overall sensitivity is 81% which indicates that 13/16 moderate/severe curves were accurately classified on the basis of the ST parameters. Moreover, 15/19 mild curves were classified correctly with a specificity of 79%. This suggests that 79% of the mild curves could have avoided an X-ray examination based on the algorithm introduced in this study. Consequently, the overall accuracy in classifying the severity of T-TL curves based on this method is 80%.

Table 3-2- Severity classification results for the Testing group. The (+) and (-) in the tables represent the Progression and Non-progression groups, respectively.

T-TL		Radiograph (+)	Radiograph (-)
ST	(+)	13	4
	(-)	3	15
Accuracy		Sensitivity	Specificity
80%		81%	79%

L		Radiograph (+)	Radiograph (-)
ST	(+)	14	8
	(-)	1	9
Accuracy		Sensitivity	Specificity
72%		93%	53%

With the same procedure, 20% of L curves were stored in the Testing group (32 curves) leaving 136 curves in Training group. The optimum values for the number of neighbours in the first and second iterations, respectively, were found to be k_1=18 and k_2=5.

Of the 32 L curves in the Testing group, 15 were moderate/severe and 17 were mild based on radiographic measures. 14/15 moderate/severe curves were correctly identified with a sensitivity of 93% (Table 2). Furthermore, 9/17 of the mild curves were diagnosed correctly for a specificity of 53% suggesting that more than half of the mild curves could have avoided an X-ray examination. The overall accuracy of the proposed method for L curves was 72%.

3.4.2 Curve progression

The curve progression was studied for those patients who have follow-up scans (134 curves) with ΔRMS and $\Delta MaxDev$ being the independent variables. Twenty-seven curves were included in the Testing group and 107 curves were included in the Training group. The optimum value for k_1 was found to be 17, i.e. 17 curves with the lowest absolute difference of ΔRMS with respect to the data point under study were used. The optimum value for k_2 was 1, indicating that the closest neighbour in terms of $\Delta MaxDev$ classifies whether the current curve experienced progression or not. 5/6 progressive curves were identified correctly (Sensitivity = 83%) and 20/21 non-

progressive curves were identified correctly (Specificity = 95%) (Table 3.) The high sensitivity confirms that the proposed method can accurately distinguish the progressive curves (low number missed) giving clinicians confidence in the method's ability to identify patients who could skip radiographs without missing treatment opportunities.

Table 3-3 - Curve progression classification results for the Testing group. The (+) and (-) in the tables represent the Progression and Non-progression groups, respectively.

		Radiograph (+)	Radiograph (-)
ST	(+)	5	1
	(-)	1	20
Accuracy		Sensitivity	Specificity
93%		83%	95%

The capability to classify the curve severity of AIS curves though using the customized k-NN algorithm was compared with previous work [64] in markerless ST (Figure 3-6). For the case of T-TL curves, the specificity in the curve severity classification showed a substantial increase compared to the previous work [64] from 58% to 79%. However, our approach failed to distinguish moderate/severe curves as well as the traditional classification tree with a decrease in sensitivity from 100% to 81%. The overall accuracy slightly improved with an increase from 77% to 80%. In the curve severity of L curves, we showed an improvement in sensitivity from 87% to 93% along with an increase in specificity from 41% to 53% compared to the previous work [64].

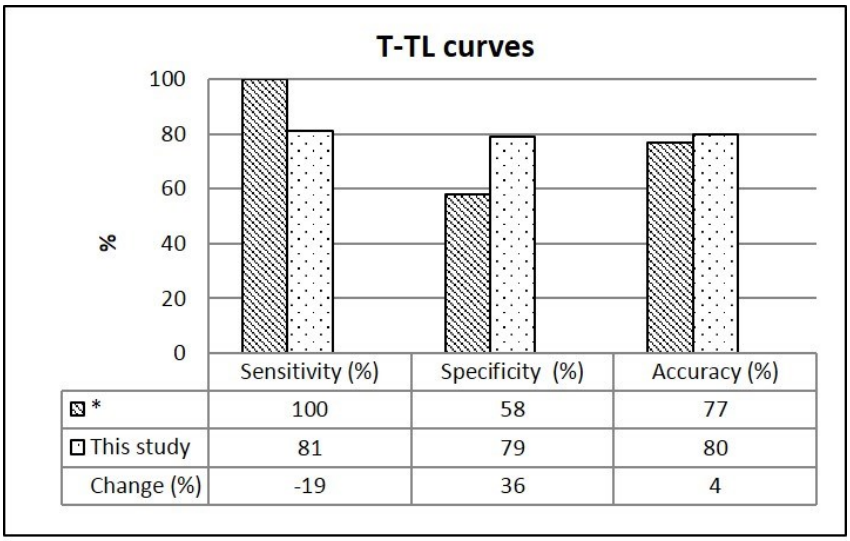

	Sensitivity (%)	Specificity (%)	Accuracy (%)
*	100	58	77
This study	81	79	80
Change (%)	-19	36	4

(a)

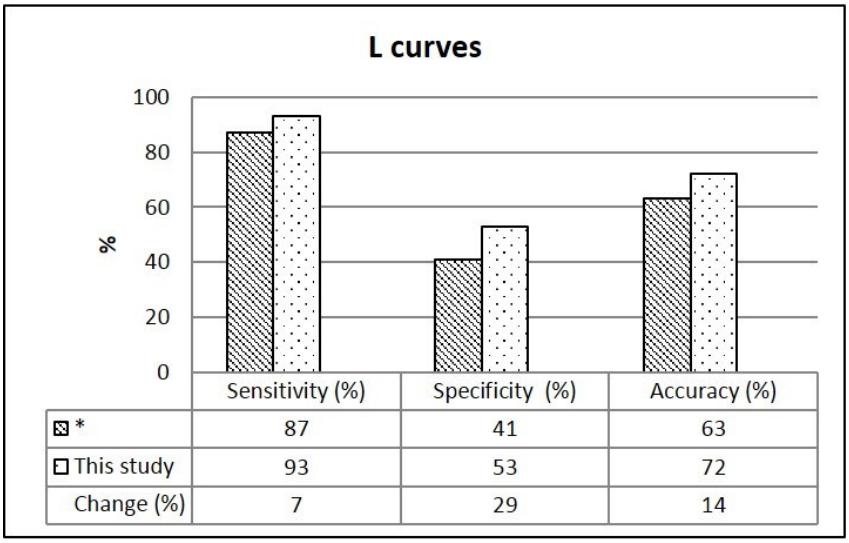

	Sensitivity (%)	Specificity (%)	Accuracy (%)
*	87	41	63
This study	93	53	72
Change (%)	7	29	14

(b)

Figure 3-6- Comparing the performance of the customized k-NN with a previous study using classification tree analysis [64] in classifying the severity for (a) T-TL and (b) L curves in the Testing group

Considering curve progression, the current method showed a substantial improvement over the previous work [64] (Figure 3-7). Progressive curves were identified with 83% accuracy, exhibiting an increase in sensitivity from 67% with the other method. Furthermore, the overall accuracy of the classifying curve progression significantly increased from 59% to 93%.

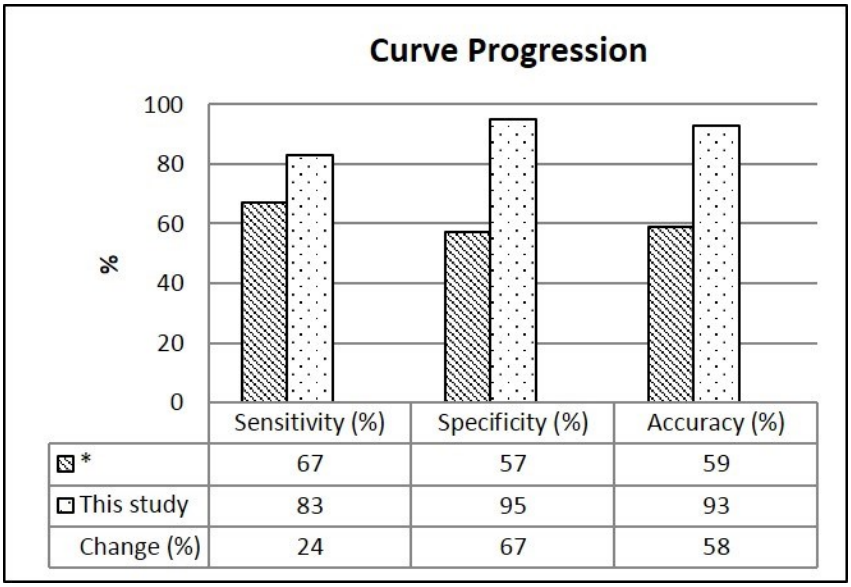

	Sensitivity (%)	Specificity (%)	Accuracy (%)
*	67	57	59
This study	83	95	93
Change (%)	24	67	58

Figure 3-7- Comparing the performance of the customized k-NN with classification tree analysis reported in a previous study [64] in classifying the progression of the scoliosis curves

3.5 Discussion and Conclusion

The motivation of the present study lies in the potential of classifying the severity and progression of curves in AIS patients based on ST thereby potentially reducing the use of radiographs. More precisely, the k-NN analysis was conducted to further minimize the risk of missing moderate/severe or progressive curves and reduce the number of mild and non-progressive curves misclassified while maximizing the sensitivity compared to the classification tree analysis previously reported in the literature [64] .

For L curve severity classification, by using the new classification method introduced in this study, sensitivity, which represents the probability of identifying moderate/severe curves, was improved from 87% to 93% compared to when using classification tree analysis. It should be noted that the only misclassification of a moderate/severe curve was specific to the only patient with a double curve, in which the upper curve in the T-TL area was detected correctly as severe. In a clinical setting, the severe T-TL curve would lead the patient to go under further X-ray investigation, thus the missed L curve would not have impacted the clinical care of the patient. In a double curve spine, having a large curvature in the T-TL section reduces the cosmetic deformity in the lumbar area, i.e. the asymmetry parameters corresponding to the L curve on the deviation contour map are smaller than they could be if there was no T-TL curve. Further investigation is required to study the interconnected effects of T-TL and L curves on a larger sample set of patients with double curves.

Another advantage of the proposed technique is the increase in the specificity of curve severity classification for lumbar curves from 41% to 53%. This increase in specificity would result in a decrease in the number of patients with mild curves being exposed to X-ray radiation. The corresponding increase in sensitivity from 87% to 93% shows that this would occur while missing even fewer moderate/severe curves requiring the clinician's attention. These results substantiate the fact that the new method is better able to diagnose L curves by improving the overall accuracy of curve severity classification from 63% to 72%. Hence, L curve severity can be assessed with higher confidence.

For T-TL curve severity, the sensitivity obtained in this study was lower than the former classification method (81% compared to 100%). The three moderate/severe curves that were inaccurately identified as mild in the k-NN classification analysis belong to patients with high body mass indices (BMI). These patients had BMI > 25 which is the standard threshold of overweight. Hence, this misclassification likely resulted from a reduction in the torso asymmetry due to the fatty tissue masking the underlying deformity.

To investigate the effect of BMI>25, all the patients meeting this criterion were eliminated from the dataset and the analysis with the same features was performed again. The sensitivity and accuracy for patients with BMI≤25 reached to 100% and 83%, respectively. In particular, all the moderate/severe curves were successfully identified by the new analysis. The modified dataset did not reveal any changes on the number of mild misclassified curves (4 curves); however, the specificity reduced to 67% due to the decrease in the number of patients in the modified dataset. The results, in particular the significant improvements of sensitivity and accuracy after excluding the subjects with BMI>25, suggests that excess body fat can considerably influence the asymmetry parameters.

In a clinical setting, if radiographs were not ordered for patients identified with a mild curve, the classification trees presented in Ghaneei et al. [64] could reduce the number of X-rays by 24% (9/37) while the customized k-NN presented here could reduce the number of X-rays by 34% (12/37). In this study, the k-NN classification correctly identified 55% (12/22) of the mild patients.

Furthermore, this study proposed a new method for monitoring AIS curves over time, which remarkably improved the accuracy of identifying curve progression. Only one curve was misclassified and considered as non-progressive after the one-year follow-up interval. For this curve, however, the increase in Cobb angle was exactly equal to 5 degrees which is on the margin between progressive and non-progressive and is within the Cobb angle measurement error. In addition, one curve was misdiagnosed as progressive when the increase in Cobb angle was actually less than 5 degrees. The increase in sensitivity from 67% to 83% compared to the previous study by Ghaneei *et al.* [64] means fewer progressive curves would be missed by using the customized k-NN classification approach. The identification of non-progression curves (specificity) also increased from 57% to 95%, demonstrating a clear advantage of the current method in terms of protecting patients against unnecessary radiographs.

In a clinical setting, if radiographs were not ordered for patients identified as non-progressive, the customized k-NN could reduce the number of X-rays by 74% (14/19) while the classification tress presented in Ghaneei *et al.* [64] could reduce the

number of X-rays by 42% (8/19). It is important to note that 100% (14/14) of the non-progressive patients in the Testing group were correctly identified by k-NN while only 57% (8/14) were identified correctly using the classification trees [64]. These are clinically important results and indicate that our markerless ST technique, combined with the customized k-NN classification method is far superior to previous methods in terms of the ability to reduce the X-ray exposure for AIS patients.

One of the limitations of this study is that some curves came from the same patients which may lead to data overfitting. The results presented here can be further validated on a larger sample of patients.

The devised methodology in the present work provided a substantially improved accuracy compared to literature. Further improvements may be achieved by increasing the Training group size. Future work will focus on further investigation of double curve spinal deformities as well as patients with BMI greater than 25. Also, in future studies, BMI can be applied as an independent variable along with *RMS* and *MaxDev* in the analysis. We are confident that our research will serve as a base for future studies on AIS analysis based on ST monitoring and we have shown that this method has the potential to significantly reduce the number of X-rays required during clinical follow-up of patients with AIS.

4

Summary and Conclusions

4.1 Conclusion

To meet the given objectives as mentioned in the introduction chapter, this study proposed a modification to the previously developed 3D markerless asymmetry analysis [3, 51] using a new asymmetry threshold. We have succeeded in eliminating the manual step which was necessary for isolating the deviation patches in some patients. Before automating the isolation step, after creating the deviation contour map and isolating the deviation patches, an expert was needed to double check the patch isolation results and to isolate the patch manually when it was necessary. That is because some of the patches could extend to the anterior section of the torso and around the armpits, or the boundaries between the deviation patches in ST scans of patients with a double or triple scoliosis curves were not properly separated. To the best of our knowledge, no repeatable instructions were provided for the manual separation which led to questioning the repeatability of the patch isolation. By using the modified method an operator would be able to automatically perform the ST

analysis process through repeatable and reliable procedure. The proposed approach was able to accurately classify 95% of moderate/severe curves and save 35% of mild curves which caused patients to get exposed to X-ray. In this regard, the probability of missing a moderate/severe curve is significantly low. The strength of our work lies in monitoring curve progression status in which 75% of progressive curves were correctly identified, i.e. the probability of missing curves with progression was 10% lower than the original method [29]. Also, 59% of curves without clinically progression ($\Delta CA < 5°$) during 12±3 months were identified. The results are conservative such that smaller number of radiographs would be saved, however the risk of missing a progressed curve would be decreased while the probability of diagnosing the moderate/severe curves remained as high as before. The findings of this work were submitted in a form of journal paper to the Journal of Medical & Biological Engineering & Computing.

The second chapter was submitted to the Journal of computer methods in biomechanics and biomedical engineering which demonstrates the new method, Nested attribute neighbourhood classifier, instead of traditional classification trees to use the deviation contour map in AIS management. As stated in the Chapter 3, the Nested attribute neighbourhood classifier was assessed as a successful approach for using markerless ST for decision makers in AIS management. Considerable progress has been made in classifying the curve severity of curves located in the L section with regard to increase the specificity from 41% to 72% and sensitivity from 87% to 93% and compare to applying previous tree method [64].The results show a dramatic increase of the sensitivity (from 67% to 83%) and specificity (from 57% to 95%) in monitoring curve progression. The customized k-NN method misclassified the curves of a few patients. ThreeT-TL curves that were misclassified belonged to patients with BMI>25, while one L curve belonged to a double curve patient. Furthermore, the corresponding change in the Cobb angle of one progressive curve, which was misclassified, was 5 degrees which is on the margin between progressive and non-progressive and is within the Cobb angle measurement error.

Overall, if clinicians decided not to expose patients with a mild AIS status or no progression in their spinal curve to unnecessarily radiation by applying the customized

k-NN, 55% of patients with mild curve and all the patients with no curve progression can be saved from being exposed to X-ray.

In conclusion, the findings of this study indicate that by using the new method for the severity classification and monitoring AIS, moderate/severe or progressed curves would not be missed if caution is taken in the following conditions:

- Patients with BMI>25
- Patients with double curves
- Changing in Cobb angle is approximately 5 degrees.

4.2 Limitations and Future Work

We are aware that our research may have some limitations. Undoubtedly, the more data we have, the better accuracy that can be obtained. Despite of having great number of data for statistical analysis, it has to be acknowledged that the Training group only contained 39 patients with curve progression which may not fully capture the full spectrum of scoliosis curve types, such as single and double curves. However, using the Nested attribute neighbourhood classifier can be simply improved by adding more data to the Training group which would result in decreasing the probability of errors in classification output. In our analysis, only the *RMS* and *MaxDev* were used as variables for classification. Further studies could consider other ST parameters such as curvature of the back valley [60], trunk axial rotation [61]. Given these limitations, this research still serves as a base for future studies on AIS analysis based on ST monitoring. Our results shown that combining our analysis method with the Nested attribute neighbourhood classifier has the potential to significantly reduce the number of X-rays required during clinical follow-up of AIS patients.

Bibliography

[1] D. A. Hoffman, J. E. Lonstein, M. M. Morin, W. Visscher, B. S. H. 3rd, and J. D. B. Jr, “Breast cancer in women with scoliosis exposed to multiple diagnostic x rays,” *J. Natl. Cancer Inst.*, vol. 81, no. 17, pp. 1307–1312, Sep. 1989.

[2] J. G. Thometz, R. Lamdan, X. C. Liu, and R. Lyon, “Relationship between Quantec measurement and Cobb angle in patients with idiopathic scoliosis,” *J. Pediatr. Orthop.*, vol. 20, no. 4, pp. 512–516, 2000.

[3] A. Komeili, L. Westover, E. C. Parent, M. Moreau, M. El-Rich, and S. Adeeb, “Surface topography asymmetry maps categorizing external deformity in scoliosis.,” *Spine J.*, vol. 14, no. 6, p. 973–983.e2, Jun. 2014.

[4] G. C. Lam, D. L. Hill, L. H. Le, J. V Raso, and E. H. Lou, “Vertebral rotation measurement: a summary and comparison of common radiographic and CT methods,” *Scoliosis*, vol. 3, p. 16, Nov. 2008.

[5] S. Sharma *et al.*, “A PAX1 enhancer locus is associated with susceptibility to idiopathic scoliosis in females,” *Nat. Commun.*, vol. 6, pp. 1–10, 2015.

[6] L. G. Lenke and M. B. Dobbs, “Management of Juvenile Idiopathic Scoliosis,” *J. Bone {&} Jt. Surg.*, vol. 89, no. suppl{_}1, pp. 55–63, Feb. 2007.

[7] J. A. Farady, “Current principles in the nonoperative management of structural adolescent idiopathic scoliosis,” *Phys. Ther.*, vol. 63, no. 4, pp. 512–523, Apr. 1983.

[8] J. Sales de Gauzy, Q. Ballouhey, C. Arnaud, H. Grandjean, and F. Accadbled, “Concordance for curve type in familial idiopathic scoliosis: a survey of one hundred families.,” *Spine (Phila. Pa. 1976).*, vol. 35, no. 17, pp. 1602–1606, 2010.

[9] D. Berwick, “Scoliosis screening,” *Pediatr Rev*, pp. 238–247, 1984.

[10] B. V Reamy and J. B. Slakey, “Adolescent idiopathic scoliosis: review and current concepts,” *Am. Fam. Physician*, vol. 64, no. 1, pp. 111–116, Jul. 2001.

[11] R. J. Cobb, “Outline for study of scoliosis.,” *American academy of orthopaedic surgeons*. pp. 261–275, 1948.

[12] P. N. Soucacos *et al.*, “Assessment of curve progression in idiopathic scoliosis,” *Eur. Spine J.*, vol. 7, no. 4, pp. 270–277, 1998.

[13] L. Ramirez, N. G. Durdle, V. J. Raso, and D. L. Hill, “A support vector machines classifier to assess the severity of idiopathic scoliosis from surface topography,” *Inf. Technol. Biomed. IEEE Trans.*, vol. 10, no. 1, pp. 84–91, 2006.

[14] T. N. Theologis, J. C. Fairbank, A. R. Turner-Smith, and T. Pantazopoulos, “Early detection of progression in adolescent idiopathic scoliosis by measurement of changes in back shape with the Integrated Shape Imaging System scanner,” *Spine (Phila. Pa. 1976).*, vol. 22, no. 11, p. 1223--7; discussion 1228, Jun. 1997.

[15] S. Ulkatan, M. Neuwirth, F. Bitan, C. Minardi, A. Kokoszka, and V. Deletis, “Monitoring of scoliosis surgery with epidurally recorded motor evoked potentials (D wave) revealed false results,” *Clin. Neurophysiol.*, vol. 117, no. 9, pp. 2093–2101, 2006.

[16] K. Bridwell and M. R. DNP, “Spine Universe, Anatomical Planes of the Body.” [Online]. Available: https://www.spineuniverse.com/anatomy/anatomical-planes-body.

[17] E. Mihai, “Runner Click, Scoliosis: Curvature of the Spine.” [Online]. Available: https://runnerclick.com/scoliosis-curvature-spine-sma/.

[18] “USA SYNCHRO, Understanding Neutral Spine Position and the Core Muscles.” [Online]. Available: https://www.teamusa.org/USA-Synchronized-Swimming/Features/2013/July/24/Understanding-Neutral-Spine-Position-and-the-Core-Muscles.

[19] M. Tones, N. Moss, and D. W. P. Jr, “A review of quality of life and psychosocial issues in scoliosis,” *Spine (Phila. Pa. 1976).*, vol. 31, no. 26, pp. 3027–3038, Dec. 2006.

[20] X. C. Liu, J. G. Thometz, R. M. Lyon, and J. Klein, “Functional classification of patients with idiopathic scoliosis assessed by the Quantec system: a discriminant functional analysis to determine patient curve magnitude,” *Spine (Phila. Pa. 1976).*, vol. 26, no. 11, p. 1274--8; discussion 1279, Jun. 2001.

[21] M. Gstoettner, K. Sekyra, N. Walochnik, P. Winter, R. Wachter, and C. M. Bach, “Inter- and intraobserver reliability assessment of the Cobb angle: manual versus digital measurement tools,” *Eur. Spine J.*, vol. 16, no. 10, pp. 1587–1592, Oct. 2007.

[22] P. O. Ajemba, N. G. Durdle, and V. J. Raso, “Characterizing torso shape deformity in scoliosis using structured splines models,” *IEEE Trans. Biomed. Eng.*, vol. 56, no. 6, pp. 1652–1662, Jun. 2009.

[23] J. L. Jaremko *et al.*, “Genetic algorithm-neural network estimation of cobb angle

from torso asymmetry in scoliosis," *J. Biomech. Eng.*, vol. 124, no. 5, pp. 496–503, Oct. 2002.

[24] P. O. Ajemba, N. G. Durdle, D. L. Hill, and V. J. Raso, "A Torso-Imaging System to Quantify the Deformity Associated With Scoliosis," *Instrum. Meas. IEEE Trans.*, vol. 56, no. 5, pp. 1520–1526, 2007.

[25] C. J. Goldberg, M. Kaliszer, D. P. Moore, E. E. Fogarty, and F. E. Dowling, "Surface topography, Cobb angles, and cosmetic change in scoliosis," *Spine (Phila. Pa. 1976).*, vol. 26, no. 4, pp. E55--63, Feb. 2001.

[26] A. Komeili, L. Westover, E. C. Parent, M. El-Rich, and S. Adeeb, "Correlation between a Novel Surface Topography Asymmetry Analysis and Radiographic Data in Scoliosis," *Spine Deform.*, vol. 3, no. 4, pp. 303–311, 2015.

[27] A. Hong *et al.*, "Surface Topography Classification Trees for," vol. 41, no. 0, pp. 1–8, 2016.

[28] A. Hong *et al.*, *Surface Topography Classification Trees for Assessing Severity and Monitoring Progression in Adolescent Idiopathic Scoliosis (AIS)*, vol. 41, no. 0. 2016.

[29] A. Komeili, L. Westover, E. C. Parent, M. El-Rich, and S. Adeeb, "Monitoring for idiopathic scoliosis curve progression using surface topography asymmetry analysis of the torso in adolescents," *Spine J.*, vol. 15, no. 4, pp. 743–751, Apr. 2015.

[30] Sarunas Raudys, *Statistical and Neural Classifiers, An Integrated Approach to Design*. Springer-Verlag London, 2001.

[31] D. a. Freedman, *Statistical Models: Theory and Practice*. Cambridge University Press, 2009.

[32] M. Strano and B. M. Colosimo, "Logistic regression analysis for experimental determination of forming limit diagrams," vol. 46, pp. 2005–2007, 2006.

[33] S. K. Palei and S. K. Das, "Logistic regression model for prediction of roof fall risks in bord and pillar workings in coal mines : An approach," vol. 47, pp. 2008–2010, 2009.

[34] D. W. Hosmer and S. Lemeshow, "Applied Logistic Regression," *Wiley Series in Probability and Sattistics*, no. 1. p. 373, 2000.

[35] T. K. Ho, "The Random Subspace Method for Constructing Decision Forests," vol. 20, no. 8, pp. 832–844, 1998.

[36] T. Kohonen, "Learning Vector Quantization," in *The Handbook of Brain Theory and Neural Networks*, M. A. Arbib, Ed. Learning Vector Quantization: MIT Press, 1998, pp. 537–540.

[37] N. S. Altman, “An introduction to kernel and nearest-neighbor nonparametric regression,” *Am. Stat.*, vol. 46, no. 3, pp. 175–185, 1992.

[38] D. W. Aha, D. Kibler, and M. K. Albert, “Instance-Based Learning Algorithms,” *Mach. Learn.*, vol. 6, no. 1, pp. 37–66, 1991.

[39] E. Alpaydm, *Introduction to Machine Learning Second Edition*. The MIT Press.

[40] B. V Dasarathy, *Nearest Neighbor (NN) Norms : NN Pattern Clasification Techniques*. Los Alamitos (Cal.): IEEE Computer Society Press, 1991.

[41] E. J. Rogala, D. S. Drummond, and J. Gurr, “Scoliosis: incidence and natural history. A prospective epidemiological study,” *J. Bone {&} Jt. Surg.*, vol. 60, no. 2, pp. 173–176, 1978.

[42] J. W. Roach *et al.*, “Adolescent idiopathic scoliosis.,” *Lancet*, vol. 371, no. 9623, pp. 1527–37, 2008.

[43] T. Thulbourne and R. Gillespie, “The rib hump in idiopathic scoliosis. Measurement, analysis and response to treatment,” *J. bone Jt. surgery.British Vol.*, vol. 58, no. 1, pp. 64–71, Feb. 1976.

[44] C. M. Ronckers, M. M. Doody, J. E. Lonstein, M. Stovall, and C. E. Land, “Multiple diagnostic X-rays for spine deformities and risk of breast cancer,” *Cancer Epidemiol. biomarkers {&} Prev. a Publ. Am. Assoc. Cancer Res. cosponsored by Am. Soc. Prev. Oncol.*, vol. 17, no. 3, pp. 605–613, Mar. 2008.

[45] M. M. Doody, J. E. Lonstein, M. Stovall, D. G. Hacker, N. Luckyanov, and C. E. Land, “Breast cancer mortality after diagnostic radiography: findings from the U.S. Scoliosis Cohort Study,” *Spine (Phila. Pa. 1976).*, vol. 25, no. 16, pp. 2052–2063, Aug. 2000.

[46] C. M. Ronckers, C. E. Land, J. S. Miller, M. Stovall, J. E. Lonstein, and M. M. Doody, “Cancer Mortality among Women Frequently Exposed to Radiographic Examinations for Spinal Disorders,” *Radiat. Res.*, vol. 174, no. 1, pp. 83–90, Jul. 2010.

[47] C. L. Nash, E. C. Gregg, R. H. Brown, and K. Pillai, “Risks of exposure to X-rays in patients undergoing long-term treatment for scoliosis,” *J. Bone {&} Jt. Surg.*, vol. 61, no. 3, pp. 371–374, Apr. 1979.

[48] A. R. Levy, M. S. Goldberg, N. E. Mayo, J. A. Hanley, and B. Poitras, “Reducing the lifetime risk of cancer from spinal radiographs among people with adolescent idiopathic scoliosis,” *Spine (Phila. Pa. 1976).*, vol. 21, no. 13, p. 1540--7; discussion 1548, Jul. 1996.

[49] G. M. Ardran, R. Coates, R. A. Dickson, A. Dixon-Brown, and F. M. Harding, “Assessment of scoliosis in children: low dose radiographic technique,” *Br. J.*

Radiol., vol. 53, no. 626, pp. 146–147, Feb. 1980.

[50] S. Don, “Radiosensitivity of children: potential for overexposure in CR and DR and magnitude of doses in ordinary radiographic examinations,” *Pediatr. Radiol.*, vol. 34 Suppl 3, pp. S167--72--41, Oct. 2004.

[51] E. Hierholzer and W. Frobin, “Rasterstereography measurement and curvature analysis of the body surface of patients with spinal deformities. In: Moreland MS, Pope MH, Armstrong GWD (eds) Moire,” New York: Pergamon Press, 1981, pp. 267–276.

[52] T. N. Theologis, R. J. Jefferson, A. H. Simpson, A. R. Turner-Smith, and J. C. Fairbank, “Quantifying the cosmetic defect of adolescent idiopathic scoliosis.,” *Spine (Phila. Pa. 1976).*, vol. 18, no. 7, pp. 909–912, 1993.

[53] A. Komeili *et al.*, “Assessment of torso deformities using 3D markerless asymmetry analysis and its clinical applications,” *Scoliosis*, vol. 8, no. Suppl 2, p. O25, 2013.

[54] J. L. Jaremko *et al.*, “Estimation of spinal deformity in scoliosis from torso surface cross sections,” *Spine (Phila. Pa. 1976).*, vol. 26, no. 14, pp. 1583–1591, Jul. 2001.

[55] S. Hill *et al.*, “Assessing asymmetry using reflection and rotoinversion in biomedical engineering applications.,” *Proc. Inst. Mech. Eng. H.*, vol. 228, no. 5, pp. 523–529, 2014.

[56] D. L. Hill *et al.*, “Evaluation of a laser scanner for surface topography,” *Stud. Health Technol. Inform.*, vol. 88, pp. 90–94, 2002.

[57] X.-H. Zhou, D. K. McClish, N. A. Obuchowski, Electronic Book Collection., and Wiley InterScience (Online service), *Statistical methods in diagnostic medicine*. Wiley, 2011.

[58] C. Gross, M. Gross, and Kuschner, “Error analysis of scoliosis curvature measurement,” *Publ. Hosp. Jt. Dis. Orthop. Inst. Ctry. Publ. United States NLM ID 8207779 Publ. Model Print Cited Mediu. Print ISSN 0883-9344 Link. ISSN 08839344 NLM ISO Abbr. Bull Hosp Jt Dis Orthop*, vol. 43, no. 2, pp. 171–7, 1983.

[59] J.-W. He *et al.*, “Accuracy and Repeatability of a New Method for Measuring Scoliosis Curvature,” *Spine (Phila. Pa. 1976).*, vol. 34, no. 9, pp. E323–E329, Apr. 2009.

[60] J. Thériault, F. Cheriet, and F. Guibault, “Automatic Detection of the Back Valley on Scoliotic Trunk Using Polygonal Surface Curvature,” in *Image Analysis and Recognition*, Berlin, Heidelberg: Springer Berlin Heidelberg, 2008, pp. 779–788.

[61] L. Samuelsson and L. Noren, “Trunk rotation in scoliosis. The influence of curve type and direction in 150 children,” *Acta Orthop. Scand.*, vol. 68, no. 3, pp. 273–276, Jun. 1997.

[62] G. Duval-Beaupere, A. Lespargot, and A. Grossiord, “Scoliosis and trunk muscles,” *J. Pediatr. Orthop.*, vol. 4, no. 2, pp. 195–200, Mar. 1984.

[63] C. Ho *et al.*, “Asymmetry Assessment Using Surface Topography in Healthy Adolescents,” pp. 1436–1454, 2015.

[64] M. Ghaneei, A. Komeili, Y. Li, E. Parent, and S. Adeeb, “3D Markerless Asymmetry Analysis in the Management of adolescent idiopathic scoliosis,” *Med. Biol. Eng. Comput.*

[65] L. Rokach and O. Maimon, *Data Mining with Decision Trees: Theory and Applications*, 2nd ed. World Scientific Publishing Co. Pte. Ltd 5 Toh Tuck Link, Singapore 596224.

[66] D. Everitt, B. S., Landau, S., Leese, M. and Stahl, *Miscellaneous Clustering Methods, in Cluster Analysis*, 5th ed. UK, 2011.

[67] J. Wang, P. Neskovic, and L. N. Cooper, “Neighborhood size selection in the k -nearest-neighbor rule using statistical confidence,” vol. 39, pp. 417–423, 2006.